DEVELOPMENT OF AN ELECTRIC TRICYCLE WITH ADJUSTABLE WHEEL CAMBER

BY

MUSAWA, Jamilu Shehu
MEng /SEET/2017/7079

DEPARTMENT OF MECHANICAL ENGINEERING

FEDERAL UNIVERSITY OF TECHNOLOGY,

MINNA

JANUARY, 2022

DEVELOPMENT OF AN ELECTRIC TRICYCLE WITH ADJUSTABLE WHEEL CAMBER

BY

MUSAWA, Jamilu Shehu
MEng /SEET/2017/7079

A THESIS SUBMITTED TO THE POSTGRADUATE SCHOOL, FEDERAL UNIVERSITY OF TECHNOLOGY, MINNA, NIGERIA
IN PARTIAL FULFILLMENT OF THE REQUIREMENTS FOR THE AWARD OF THE DEGREE OF MASTER OF ENGINEERING (M Eng) IN MECHANICAL ENGINEERING (DESIGN AND SOLID MECHANICS)

JANUARY, 2022

ABSTRACT

People with locomotive disabilities find it difficult to access public and social services and functions due to mobility issues. To have a successful rehabilitation program, an active lifestyle must be encouraged. Many locomotive assistive device variants were developed to accomplish this. The disabled tricycle is one of those devices that is commonly found in Nigeria. Tricycles are inherently unstable at high speeds and during manoeuvres, raising safety concerns. As efforts to increase the speed of tricycles used by the disabled are increased through the use of electric motors, the need to investigate their stability as speed increases has become an important safety concern. Despite the fact that there is a large body of research on three wheelers, active safety systems on these vehicles were previously ignored. The dynamic stability and control of larger three-wheel vehicles, such as auto rickshaws, were prioritized, while smaller vehicles, such as the disabled tricycle, were largely ignored. The aim of this study was to improve the stability of tricycles used by the disabled. To improve stability, geometric parameters and weight distribution were carefully chosen using steady state cornering equations, tire cornering stiffness, and understeer gradient. The kinematic bicycle model was modified for use on tricycles with delta designs. An electric-powered tricycle with adjustable wheel camber was developed. For rollover analyses, a quasi-static rollover model was used. Rollover tests were performed with various radii and camber angles. Theoretical analyses were compared to practical test results. To determine the handling characteristic, a constant radius test with a 15 m radius and different wheel camber angle adjustments of 0^o, 5^o, 10^o and 15^o was performed. At a maximum camber angle of 15^o, only a maximum speed of 17 km/h was achieved without the risk of tipping over at a radius of 15 m. As a result, the understeer gradient could not be determined due to insufficient steering angle measurement and speed readings. Wheel camber was found to improve stability, with maximum speeds of 10 km/h at 0^o camber angle and 24 km/h at 15^o camber angle all tested within a 30 m radius turn. It was observed that while camber angle improved stability of the tricycle, the calculated rollover threshold is significantly higher than the actual values. Tricycle dimensions have a large impact on stability and handling response. The very narrow dimensions of the tricycle affected the stability and handling response, as indicated by both tests, consequently, policy framework is required to regulate usage, design and manufacture to achieve desired user safety.

TABLE OF CONTENTS

LIST OF FIGURES

LIST OF PLATES

LIST OF TABLES

ABBREVIATIONS, GLOSSARIES AND SYMBOLS

W= total vehicle weight

g= acceleration due to gravity (m/s^2)

a=longitudinal acceleration (m/s^2)

a_y = Lateral acceleration (g)

d= Deceleration (m/s^2)

V= forward speed of the vehicle (m/s)

R= Radius of the turn (m)

δ= Steering angle (Deg)

α= Slip angle (Deg)

C= Cornering stiffness (N/Deg)

K= Understeer gradient

F_y= Lateral force (N)

F_s=Side force (N)

L= Wheel base (m)

l_1= Length from CG forward to the front axle (m)

l_2= Length from CG rearward to the rear axle (m)

h= Vehicle CG height from ground level (m)'

A= Inertia vector due to longitudinal acceleration

D= Inertia vector due to braking

E= Inertia vector due to lateral acceleration

Z= Resultant vector of A or D and E

γ = angle between line drawn from the centre of curvature to the vehicle's centre of mass andthe line drawn from the centre of curvature to the vehicle's rear axle.

θ= angle between the centre line of the vehicle to the tipping axis, TT.

ϕ= angle between resultant vector Z and the x axis.

β= angle between resultant vector Z and the line drawn perpendicular to the tipping axis through

the mass centre of the tricycle and the rear wheels.

CG= Centre of Gravity

UNICEF= United Nations International Children's Emergency Fund

WHO = World Health Organization

CRPD = Convention on the Rights of Persons with Disabilities

PTW = Powered Two and Three Wheelers

PW = Powered Wheelchair

SW = Smart Wheelchair

UNDP = United Nation Development Project

CHAPTER ONE

1.0 INTRODUCTION

1.1 Background to the Study

In Nigeria, tricycles are a popular mode of transportation for those with mobility issues. They are utilized to get to public venues in towns and rural areas, such as markets, schools, religious centres, places of work, hospitals, and so on. These hand crank designs are limited in range and speed as they require much effort from the user and are also difficult to manoeuvre due to larger turning radius compared to the wheelchair.

In this work, an electric hub motor on a 20 by 2.125 bicycle tire was used to replace human effort to increase range and speed. According to Kooijman *et al*. (2008), the properties of a bicycle tire are of no consequence at speeds below 21 km/h. The properties of bicycle tire, notably cornering stiffness and camber stiffness, have been found to influence handling and stability (Dressel & Rahman, 2013). Windes and Archibald (2013) also stated that tire properties such as cornering stiffness and camber stiffness have a strong influence on the stability and handling of light alternative vehicles. However, there is not much data on the tire properties for the available bicycle tires in the market.

Three wheel vehicles are popular but due to their narrow and light design they are not very stable during harsh manoeuvres and at high speed (AZadieh, 2014). The stability of three wheel vehicles can be improved from the design stage by giving thoughtful considerations to the location of the Centre of gravity (CG) and the dimensions of the wheelbase and wheel track (Starr, 2006).

In this work, equations for the conditions for handling response and lateral stability were established using steady state cornering equations and quasi static rollover model for a tricycle with delta design. The major parameters that are significant to stability are the understeer

gradient, wheelbase, wheel track, CG location. The understeer gradient, which is a key factor in defining a vehicle's handling reaction, is influenced by weight distribution and tire cornering stiffness. The understeer gradient was improved by giving the rear wheels a camber angle.

Due to mobility inconveniences, people with locomotive disabilities find it difficult to access public services such as health care, education, skills acquisition, labour market and other social services. According to the United Nations International Children's Emergency Fund (UNICEF), 95 percent of disabled children in developing nations are out of school, and 90 percent of them will not receive an education in their lifetime. Nigeria has an estimated 25 million people living with disabilities (Smith, 2011). According to Smith (2011), mobility is one of the most common disabilities in Kogi and Niger states, with about 32 percent and half of the respondents having no education, 20 percent having primary, 8 percent secondary, and 2 percent tertiary education, and a third of them (1093 respondents) being under 21 years of age and having no occupation.

To have a successful rehabilitation program an active life style must be encouraged. To achieve this, many variants of assistive devices for people with locomotive disabilities, were developed. These devices allow them to perform daily activities of life thereby improving their quality of life. The use of assistive devices helps them maintain, significantly, an independent life style and make their roles more productive in society (Ebrahimi *et al.,* 2016).

Wheelchairs are excellent mobility devices for the disabled and have attracted a lot of interest from the public, engineers, researchers and medical practitioners. It has become the global symbol for handicapped access (Mclaurin, 1990)**.** They easily navigate paved ways and can be used indoors. Its use is well supported by making public buildings wheelchair friendly through the use of ramps and lifts. However, with all its versatility the wheelchair is limited especially in most developing and under developed countries. It cannot be used to travel long distances

and over rough terrains. Due to their light and ultra-light designs, they fail to be rugged and durable for sustained usage in most developing countries **(**Winter, 2006). These limitations have spun a growing interest in wheelchair research and other assistive technologies. Some of these are developments in powered wheelchair, wheelchair attachment to form a tricycle, folding wheelchair, the hand tricycle and many others.

The commonly found tricycles in African countries like Tanzania and Kenya, similar to those in Nigeria, can be adapted for long distance travel and also used on rough terrains(Winter, 2006). From observation, most are simply fabricated using available parts from old bicycles without any engineering design considerations, thus making it impossible to meet safety requirements and expectations of the intended users.

There is a wide body of research on mobility assistive devices globally though this has not really impacted the lives of people with impaired mobility in Nigeria. A report by United Nations Development Project (UNDP) showed that local production of wheelchairs in Africa is below 1percent of the demand for wheelchairs in the continent (Winter, 2009).

One of the Sustainable Development Goals (SDG 11, target 11.2) is to provide access to safe, affordable, accessible, and sustainable transportation systems for all, as well as to improve road safety, particularly by expanding public transportation, with special attention paid to the needs of those in vulnerable situations, such as women, children, people with disabilities, and the elderly.

1.2 Statement of the Research

Nigeria has over 25 million disabled individuals (World Health organisation, WHO, 2011), and it ratified the United Nations Convention on the Rights of Persons with Disabilities (CRPD) in the year 2007 and its optional protocol in year 2010. The nation passed the disability rights bill in January 2019, laying the groundwork for total social inclusion for people with

disabilities. To realise this in its entirety, the development of appropriate home-grown solutions, to meet the mobility needs of people with disabilities, have to be addressed.

With increased speed, the tricycle, like other two axle vehicles having three-wheels, has stability issues. They are designed to work both outside and indoors, so they are a lot narrower. The basic characteristics that determine stability, such as wheelbase and wheel track, are constrained as a result of this. Stability has been identified among the risk factors associated with the usage of powered two and three wheel vehicles (PTW). Vehicle configuration to improve stability has been identified as one of the key measures and interventions to improve PTW safety (WHO, 2017). Given their narrow configuration, it is critical to design them for stability as well as investigate the parameters that determine stability.

1.3 Aim and Objectives of the Study

The aim of this work is to develop an electric tricycle for the disabled having higher speed and adjustable wheel camber for better handling and lateral stability.

The objectives are:

i. To enhance the stability by a well thought out location of the CG, the wheel base and wheel track dimensions, through the use of steady state equations governing handling stability and rollover stability.
ii. To determine the speeds at which rollover occur during lateral acceleration, during lateral acceleration in a turn, during braking in a turn.
iii. To carryout rollover velocity threshold tests.
iv. To carryout constant radius test to determine the understeer gradient.

1.4 Justification for the Study

There are works on tricycle development and design that seek to improve speed by focusing largely on choice of prime mover like electric motor and internal combustion engine, and source of electric power such as battery or solar. Others are limited to improving the material choice or carrying out finite element analysis of the structure.

Similar works on stability of three wheeled vehicles are largely related to lager vehicles like the common Auto rickshaw popularly known as Keke NAPEP, National Poverty Eradication Programme (NAPEP), in many parts of Nigeria, cargo tricycles and other related tricycles having longer wheelbase and wider track. Other works dealt with different configuration like the tadpole (two wheels at front, one wheel rear) or uses tires that have readily available or published tire properties which make for easier modelling.

This work is focused on improving the handling and rollover stability of the disabled tricycle with improved speed given its narrow and small dimensions that largely affect some of the parameters for stability. This work also seeks to establish the understeer gradient for such vehicles designed with bicycle tires.

1.5 Scope of the Study

The goal of this project is to create a prototype disabled tricycle with improved handling stability and rollover stability. A delta tricycle model was used with bicycle tyres and an electric hub motor. Adjustable rear wheel camber was used to improve the tricycle's stability. Theoretical analysis in this work was conducted using steady-state handling equations and quasi-static rollover models. The understeer gradient and rollover threshold were determined using the constant radius test and the rollover threshold test, respectively.

CHAPTER TWO

2.0 LITERATURE REVIEW

2.1 Theoretical Fundamentals

There are various mobility aid devices to assist people with mobility impairment. Some have been in existence for centuries and have evolved with advances in technology. Each device is designed to carter for a specific user group with a certain class of ailment.

There are many mobility assistive devices for long and short haul movement for the disabled to choose from. Garande *et al.* (2013) discussed the various technologies available and their suitability for the physically challenged. They differ in cost, manoeuvrability, ease of use, comfort and automation. Various devices used for the transportation include manual wheelchair, powered wheelchair, smart wheelchair, tricycles, retrofitted vehicles and modified cars.

2.1.1 Manual wheelchair

Wheel chairs are perhaps the most widely used mobility assistive device. It comes in wide variety of formats to meet specific needs of their users. Wheelchairs are distinctively classified into manual wheelchairs and powered wheelchairs. A wheelchair is defined by the world health organisation as “a device providing wheeled mobility and seating support for a person with difficulty in walking or moving about”. As a result, the goal of a wheelchair is to promote personal mobility. The goal of wheelchair design is to create wheelchairs that are both functional and offer enough sitting and support user’s posture without sacrificing safety, strength or durability. Consequently, designers must have a solid understanding of the target users' environments and requirements.

As mentioned by Visagie *et al*. (2015), the features of the design have to be compatible with the user's postural requirements, functional ability and environment. The importance of ensuring an optimal match between design, the user and surroundings is as crucial as it is challenging. Having variety of models to choose from makes it easier to meet the user’s needs.

Wheelchairs are designed to allow users to live an active lifestyle without compromising their health or safety. Long-term users' quality of life is influenced by two major factors: comfort and safety.

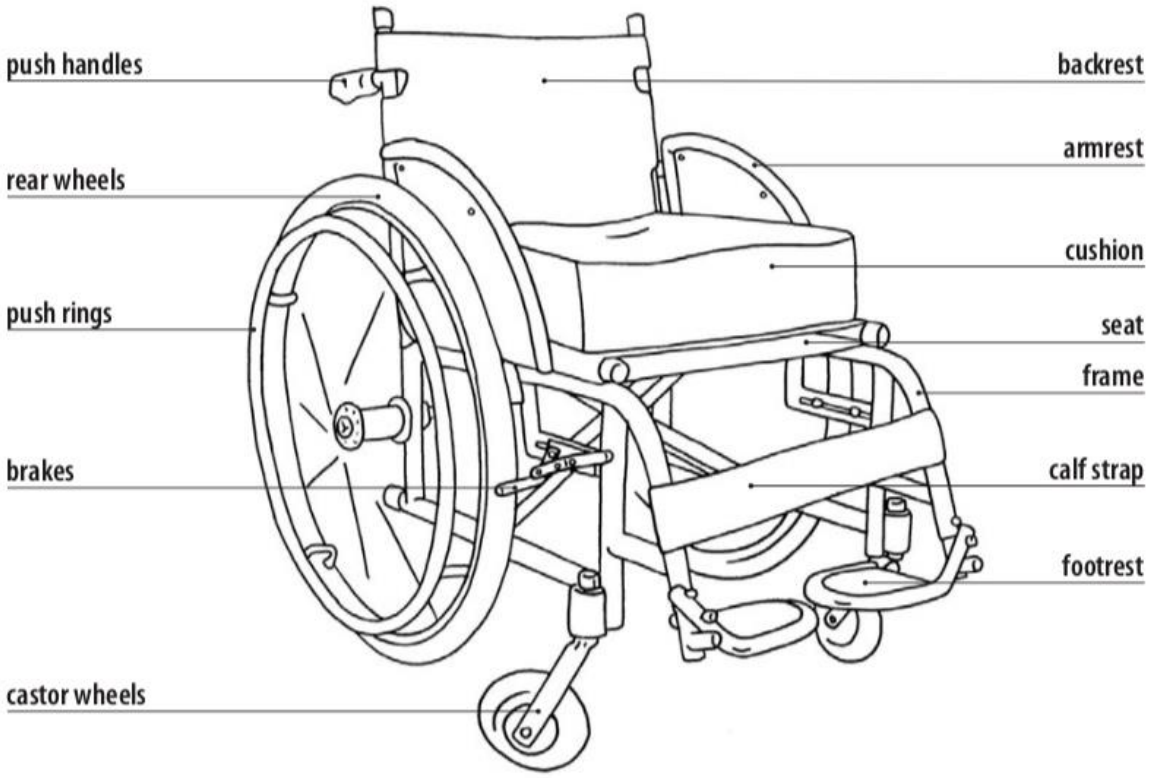

Figure 2.1: Schematic showing the functional components of a wheelchair (WHO, 2008)

According to Mclaurin (1990*)*, there are many researches targeted at greater innovations in components design of the wheelchair. The essential principles related with the functional and structural properties of wheelchairs, for example, were studied by researchers from Rehabilitation Engineering Centre at the University of Virginia. Propulsion ergonomics, seating position, rolling resistance, structural analysis, design of controller, efficiency of the motor and battery capacity are some of the topics covered. The frame, tires, and driving systems, wheels, seat, foot, and armrests are all components of a wheelchair that have various and optional characteristics. Many research efforts are focused on light materials like plastics and advanced composites in frame designs, adjustable seats and postural support, wheels and

tires to reduce maintenance and improve propulsion efficiency, improving ride through suspension system having spring constant that will provide comfort without bounce and reduce stress on the frames.

Ebrahimi *et al*. (2016) discussed overuse injuries with respect to wheelchair usage. Musculoskeletal issues may arise as a result of living in a wheelchair and using these devices for mobility for an extended period of time. Overuse injuries of the upper body have been a focus of rehabilitation study, and significant attempts have been undertaken to correct the long-term imbalance of physical strain and propulsion mechanics. Wheelchair users may choose a more sedentary lifestyle to avoid upper extremity musculoskeletal pain, which can set off a dangerous vicious cycle that leads to more secondary issues. Repetitive strain injuries mostly affect the shoulders and wrists, but they can also impact the back and neck muscles. To reduce the impact of repetitive strain on the upper limbs, several design improvements have been proposed.

The adoption of varied configurations for hand rims, rear wheel angle and inclination, and seat position have all been researched biomechanically. Aside the traditional hand rim, other propulsion means have been developed over the years. Mclaurin (1990) mentioned that the lever driven mechanisms, as shown in Plate I, have more mechanical advantage compared to the hand rim, thus in future it will become a major feature in wheel chairs. The difficulty in achieving control and manoeuvrability is a key disadvantage of levers, which has been overcome by modern designs (Mclaurin, 1990).

Jenkins *et al.* (2014) reported that crank and lever wheelchair have less straining forms of locomotion as a result of longer continuous stroking pattern. By putting the arms more in a natural segmental position, it becomes very effective in transmitting human force for wheelchair propulsion. Because of the mechanical advantage difference between the push-rim

wheelchairs and the lever-driven wheelchairs; the push-rim wheelchair has an advantage for the initial push. This is because the turning moment is greater at a bigger radius for a given muscle force. However, this is inconsistent with their findings, which show that the lever-driven wheelchair requires more force due to the usage of other groups of muscle. This causes a greater impact on performance than the push-rim wheelchair's mechanical advantage. Similarly, the lever-driven wheelchair geometry has the added benefit of making it easier to move the wheelchair at a higher speed. Human force is more efficiently transmitted by the propulsion arc length on a lever-driven wheelchair which is longer than that of a push-rim wheelchair. For the same cadence, this resulted in more effort being done and more energy being transferred into propulsion.

Plate I: Lever propelled wheelchair (www.contest.techbriefs.com, 2019)

Other wheelchair variants were developed to carter for various needs of the disabled to ensure inclusivity and improve their quality of life. The sports wheelchair, as shown in Plate II, is one

of those variant that was fully developed to fit different sporting activities. A common model was that developed by Eric Larson and his team for wheelchair sports like basket ball. Designers wanted to develop a way to give players more options for hands-free wheelchair operation. Players use their hands for propulsion, turning, braking, and handing the ball. The designers created a hands-free braking and turning technology that allows players to have more control over their chair without compromising ball handling. The design functions by reacting to the user's tilting, turning, or braking.

Plate II: Sports wheelchair (www.progressiveae.com)

Currently, the manual wheelchair is the most popular option for disabled people seeking rehabilitation and assistive mobility. This is owing to its ease of use, design, and relative low cost when compared to other mobility aids. However, it has drawbacks such as physical exertion on the user, physiological implications of long-term (or life-time) usage, restricted range and speed, and was built primarily for paved surfaces. As a result, designers have created motorized wheelchairs to address some of the issues.

2.1.2 Powered wheelchair

Powered wheelchairs (PW) are commonly known as electric powered wheelchairs (EPW). Unlike the manual wheelchair, EPWs are propelled by an electrical motor. Electric powered

wheelchairs, like those in Plate III, are designed for either indoor or outdoor usage or both. They are recommended for people who have difficulty in using the manual wheelchair due to arm, hand, shoulder or more disabling conditions and do not have strength to drive a manual wheelchair.

Mclaurin (1990) mentioned that George Klein first introduced the EPW in 1953 to assist injured veterans. The system consists of two motors with gears that drive each primary wheel separately via a rubber-faced pulley wheel, and it is powered by two 12-volt batteries. It's operated by a joystick via relays, and it's all installed on a conventional manual wheelchair. This design model dominated for a while, with the exception of incorporation of new components and making the frames sturdier. The EPW is generally seen as a modified wheelchair. This problem was addressed in a workshop, titled Wheelchair III, held in San Diego in March 1982. The powered wheelchair should be built on a powered chassis with a standard or custom seat and any other equipment that the user might require. When the powered chassis is dissociated from the anthropometric and ergonomic concerns of seating, it becomes solely an engineering challenge that may take advantage of cutting-edge engineering technology in all of its components. Significant advances were also made in electronics like power tilt, reclining systems and programmable performance settings. Joysticks are the most basic devices used to control electric wheelchairs.

Powered wheelchairs drive systems are four wheeled or six wheeled and are generally non-folding, even though folding designs exist. The location of the drive wheels is either front wheel, rear wheel, mid- or centre wheel and all-wheel drive. The drive system are either direct (gear boxes) or indirect (pulleys and drive belts). The rear wheel drive is almost preferred due to similarity with manual wheelchair in design and manoeuvrability while the centre wheel drive has gained popularity due to increased manoeuvrability. The power sources are deep

cycle rechargeable batteries mostly of lead-acid type. Lithium ion batteries are gaining popularity for such usage because they are lighter and last longer.

While there is a large amount of wheelchair research, Cooper (2012) found that there is a scarcity of study in all aspects of powered wheelchairs. However, according to Leaman and Hung (2017), there have been great efforts in research and development in powered wheelchair, smart wheelchair in particular and assistive technology, which has recorded tremendous success. Several researchers created smart wheelchairs using technologies designed originally for mobile robots to accommodate people who may find it hard or not possible to use a Powered Wheelchair. A smart wheelchair (SW) is often made up of a powered wheelchair base with a computer and sensors or a base for mobile robot with an attached seat.

Pineau *et al*. (2011), cited by Leaman and Hung (2017), claimed that the shift to wheelchairs that are cooperating with the user is as important as the transition from manual to powered wheelchairs, because it indicated more of a paradigm shift than a technological one. Some of the remarkable innovations are the autonomous wheelchair and the form of controller used by the user such as the chin control, head control and thought control.

Plate III: Smart wheelchair, a stairs climbing wheelchair and a stand up wheelchair (Leaman and Hung, 2017)

Optimization of the human-wheelchair interface (for both manual and powered wheelchairs), origins of wheelchair usage associated injury processes, practical co-robots in the natural world, and other areas of research remain elusive, according to Cooper (2012). Other areas are the wheelchair's interaction with the built environment (e.g. access to pathways, transfer guidance, design of buildings), sensing and control and effective training and assessment tools (virtual reality, virtual coaches, intelligent tutors and computerized assessment).

Sensors and processors have become quicker, cheaper, and smaller in the previous decade, according to Leamann and Hung (2017), while computer vision software is more advanced and widely obtainable like never before. Researchers created a number of prototypes, of which the most effective should combine into a modular, upgradeable system that may be sold to people who require PWs. The finest SWs should use a multi-modal interface that blends computer vision, and control by voice, touch and brain to accommodate people with several disabilities. SWs will be able to use mobile scanners to create 3D maps, employ GPS navigation, or navigate autonomously using cloud computing applications to stream and analyze sensory input in real-time. These solutions have the potential to greatly raise the standard of living for those who use PWs, but only if the people they were created to serve trust them. As a result, human factors must be considered, and Smart wheelchairs should be adaptable to the preferences of individual user, offer suitable voice feedback, and be easily mounted on any PW. Both humans and robots will interact in public settings so as to provide persons with disabilities an optimum quality of life and the prospect to reach their full human potential.

As technological advancement grow with SW so does its weight due to numerous accessories on it. This makes it difficult for transportation. Additionally the batteries have to be removed and safely stored for air transportation. SWs are not cheap due to the complex technology employed and therefore not within affordable range of many people especially in developing

countries. It will require more time to learn how to use and highly skilled technicians for maintenance.

2.1.3 Disabled tricycle

A tricycle, or trike, is a three-wheeled vehicle that is commonly used for people transportation (rickshaws), freight, recreation, and sports, as well as mobility aid for the disabled. Trikes are classified as tadpoles or deltas depending on their wheel configuration: tadpoles have two front wheels and one back wheel, while deltas have two back wheels and one front wheel. Legs or hands are typically used to push human-powered trikes. Hand crank trikes are the most prevalent type of disability trike.

A common disability mobility aid in Nigeria and many other developing nations is the hand trike. Hand trikes are more robust and preferred solutions for long distance travels on rough terrains without the more physical exertion on the user if the wheelchair were to be used. It has more speed and structural strength compared to the wheelchair. The commonly available trikes are more affordable than some wheelchairs and powered wheelchairs are prohibitively expensive for the average Nigerian user. It is easily fabricated using commonly available materials and bicycle parts. Plate IV indicates manual tricycle in Nigeria.

Plate IV: Locally made manual tricycle (www.afro.who.int)

The manual tricycle as shown in Plate IV is commonly used. Hands are utilized for cranking, braking and steering control and also reverse arrangement is available. The drive mechanism

for power transmission is a simple chain and wheel cog arrangement similar to that in a bicycle. For driving the tricycle, the user has to exert the muscular force. Plate V, VI, VII indicates different types of tricycle used by people with disabilities.

Plate V: Wheelchair trike design (www.hybrid.co.uk)

Plate VI: Armtrike AM-16 Therapeutic tricycle (www.armtrykestore.org)

`

Plate VII: Standard trike from Europe (www.flaghouse.com)

Other mobility aid devices exist for the disabled aside the wheelchair and tricycle. Common examples are mobility scooter which can also be used for the elderly, the retrofitted bike and modified cars. However, the ones that come closest to help engage the disabled in daily life activities are not surpassed by the wheelchair and tricycle. Garande *et al*. (2013) reviewed these options with their cons and pros.

2.1.4 Vehicle modelling approach

The dynamics of vehicles is concerned with vehicular movement on road surfaces. Acceleration and braking, as well as riding and turning, are the movements we are interested in. Several forces act on a vehicle exerted by the tires, gravity and aerodynamics and theses forces determine the dynamic behaviour of the vehicle (Gillespie, 1992).

Several vehicle models were developed especially in the four-wheeled vehicle class though the details and complexity is not always similar (Ferreira *et al*., 2014). Some works described only certain aspects of vehicle dynamics like lateral and longitudinal dynamics, suspension and modelling of active suspension control, aerodynamics etc.

Three-wheel vehicle dynamics have not been described extensively like four wheel vehicles (Ferreira *et al*. 2014). Houston *et al*. (1982) worked on the dynamics of different configurations of three wheeled vehicle. Three-wheel passenger vehicle stability and handling was discussed

by Valkenburgh *et al*. (1982). The work of Starr (2006) described the designing of a stable three-wheeled solar race car and three wheeled tilting vehicles were analyzed by Berote *et al*. (2008) and Amati *et al*. (2011). Ferreira *et al.* (2014) worked on the multi body dynamics of a three wheeled electric car.

The vehicle together with its structural components are investigated to establish the forces generated from each of these sources during a specific manoeuvre and trim state, as well as the vehicle's response to these forces. The method to systems modelling and the rules for describing motions was established.

2.1.5 Lumped mass model

A vehicle is made up of several components, however for the purposes of analysis, the components are assumed to move together. When the vehicle is braking or accelerating, for example, the whole vehicle reduces speed or accelerates as a single entity. As a result, it is depicted as a single lumped mass with appropriate mass and inertia parameters placed at the centre of gravity (CG). One mass for analyses concerned with braking, acceleration and turning. While sprung mass is utilized for the body and un-sprung mass is used for the wheels in ride analysis. For all motions, the point mass at the CG is dynamically identical to the vehicle itself, with corresponding rotational moments of inertia, hence the vehicle is assumed to be rigid (Gillespie, 1992).

2.1.6 SAE Vehicle coordinate system

A vehicle's motion is referenced according to the Society of Automotive Engineers (SAE) SAE J670 convention using a right-hand orthogonal coordinate system originating at the CG. As indicated in Figure 2.2, the x axis point forward in the longitudinal direction, the y axis points sideways in the lateral direction and is positive if pointed to driver’s the right hand, and the z axis points downward to the ground. Only the x-y planes are addressed in studies on handling

and directional control. In studies of ride, pitch, and roll-over stability, the z plane is taken into account.

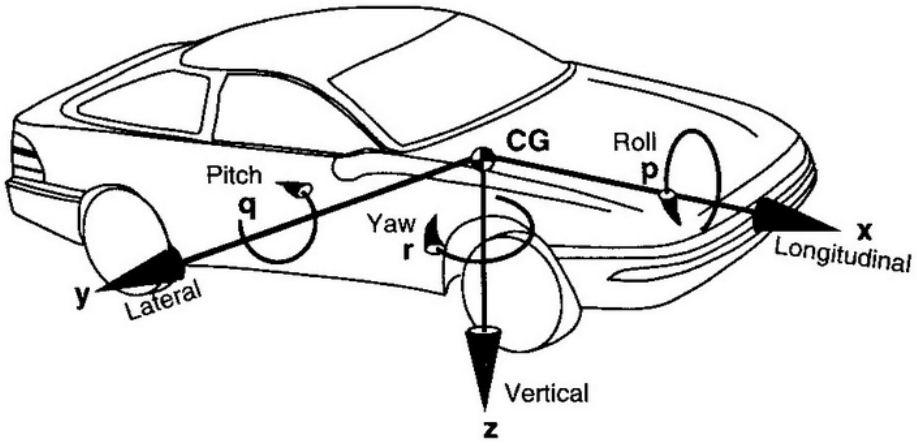

Figure 2.2: SAE Vehicle Coordinate System (Gillespie, 1992).

x- Forward along longitudinal plane of symmetry

y- Lateral, outward the right hand of the vehicle

z- Downward, with regard to the vehicle

p- Roll velocity about the X axis

q- Pitch velocity about the Y axis

r- Yaw velocity about the Z axis

The above listed velocities describe a vehicular motion with regard to the vehicle coordinate system, where the earth's fixed coordinate system is used to reference all velocities.

2.1.7 Earth fixed coordinate system

During the course of a manoeuvre, a right hand orthogonal system is utilized to determine a vehicle's attitude and trajectory. It's usually chosen to match the vehicle's fixed coordinate system, which is where the manoeuvre begins. These coordinates are:

X- Travel Forward

Y- Travel towards right

Z- Positive downward Travel (vertical)

Ψ-Heading angle (in the ground plane, the angle between x and X)

ν- Course angle (the angle between the vehicle's velocity vector and X axis)

β- Side slip angle (the angle between the vehicle's velocity vector and x axis)

2.1.8 Tire axis system

The tire characteristics have a significant impact on a road vehicle's dynamic performance. The vehicle's contact point with the road surface is the tire and it is through the tire that torque from the power-train is applied to the wheel. One of the most often utilized axis systems to analyse the forces and moments acting on a vehicle tire, especially during cornering, are the SAE J670, as shown in Figure 2.3.

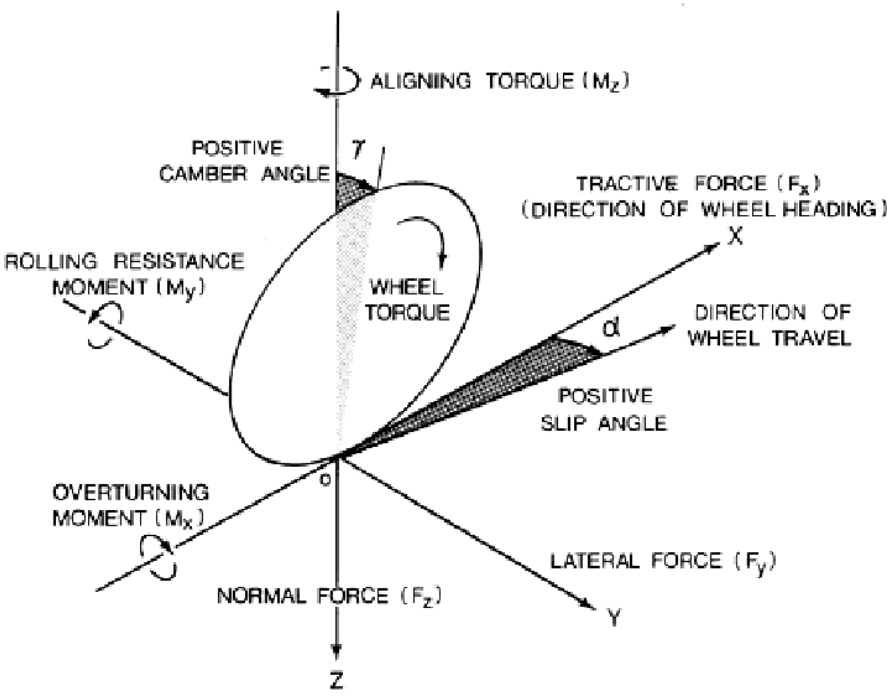

Figure2.3: Tire Axis System (Wong, 2001)

The centreline of the tire's contact patch serves as the origin of the axis system. The intersection of the wheel plane and that of the ground plane is the X axis, and the positive direction is forward. The Z axis is perpendicular to the ground plane and has a positive downward direction. The Y axis is located in the ground plane, and its direction was selected to ensure the axis system orthogonal and right-handed. From the ground, three forces and three moments act on the tire. The component in the X direction of the resulting force applied on the tire by the road is the tractive force (or longitudinal force) F_x. The component in the Y direction is lateral force F_y, while the component in the Z direction is normal force F_z. The road exerts a moment, known as, overturning moment $M_{x,}$, about the X axis on the tire. The moment about the Y axis is the rolling resistance moment M_y and aligning torque M_z, is the moment about the Z axis.

In the analysis of a rolling tire, two angles are critical: the slip angle and the camber angle. The angle formed by the wheel's directional heading and the line intersecting the wheel plane with the surface of the road is known as the slip angle. The angle formed by the XZ plane and the wheel plane is known as camber. Both angles affect the lateral force at the contact patch between the tire and the ground.

2.1.9 Vehicle handling and stability

The handling quality of a road vehicle refers to the way it responds to the driver's steering inputs and to environmental conditions like road obstructions and wind gust that affects its heading. The two concerns in vehicle handling is controlling its direction of motion and stabilizing its direction against environmental disturbances (Wong, 2001).

If the steering wheels are easy to handle, a vehicle is said to have good handling characteristics. Handling often confused with ease of cornering and turning is concerned with lateral acceleration and refers to the vehicle's ability to provide feedback to the driver in order to facilitate and improve control. Steady state behaviour, transient behaviour and resistance to rollover are the three areas that handling quality is considered (Azadieh, 2014). Longitudinal,

lateral, and yaw motions are the three primary motions that affect a vehicle's handling (translator motion along the x axis, translator motion along the y axis and rotational motion about the z axis, respectively). The vehicle body rolls (i.e. rotates about the x axis) during a turning manoeuvre, and this roll motion tends to alter the wheels heading, influencing the vehicle's handling characteristics. The vehicle's steering reaction is additionally affected by motions of the vehicle body due to bounce and pitch (translator motion along the z axis and rotational motion about the y axis, respectively). Though, these motions are only included in the analysis when the limits of handling characteristics are considered (Wong, (2001).

It is necessary to minimize pitch and roll motion for a proper handling when a vehicle is turning, braking, acceleration, and during harsh manoeuvres. It is also necessary to have a stiff chassis and suspension for a good handling quality.

2.1.9.1 *Side-slip angle*

A pneumatic tire will move along the wheel plane when not subjected to a force perpendicular to the wheel plane (side force). A lateral force arises at the contact patch when it is subjected to a side force F_s, and the tire moves along a path that is deviated from the wheel plane. The angle is known as the slip angle, α. When the wheel camber angle is zero, the lateral force (side force) created at the tire contact patch is referred to as the cornering force $F_{y\alpha}$. The link between slip angle and cornering force is critical for road vehicle directional control and stability, which can be improved by improving lateral forces on tires and controlling the steering system.

If the side load F_s is greater than the lateral force F that the tire can produce at its maximum slip angle, tire slide will occur. For a 17-inch bicycle tyre, data is available for slip angles of +3 and -3 degrees, implying that the maximum value will not be much higher. Maximum slip angles of + or - 10 degrees are plotted for automotive tires (Starr, 2006).

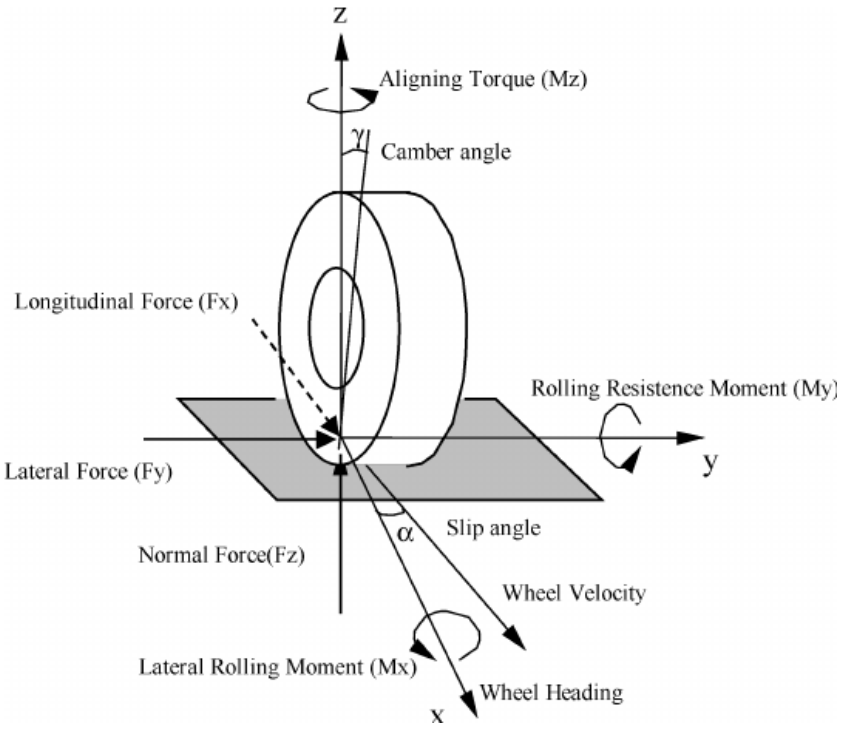

Figure 2.4: Tire forces and moments showing slip angle, (Ambrosio, 2005)

2.1.9.2 *Steady state handling behavior*

Steady state handling describes a vehicle's directional behaviour during a turn and assumes non-time changing conditions such as constant radius, constant forward speed and constant lateral acceleration. The vehicle's inertia properties are no taken into account in this form of analysis. Effects of centrifugal force acting at the CG cannot be neglected when the vehicle negotiates a turn at higher or moderate speed. Appropriate cornering forces are developed by the tires, which produce slip angles, to counteract the effects of the centrifugal force. The link between the front and rear tire slip angles has a significant impact on the vehicle's handling qualities. The pair of tires at the front and back will be represented as a single tire with double the cornering forces to simplify the study of a two axle vehicle with four wheels. The relationship between the vehicles' wheel base *L*, the turning radius *R*, the front tire's steer angle δ_f, and the front and rear tire's slip angles tires α_f and α_r may be calculated using the geometry depicted in Figure 2.5.

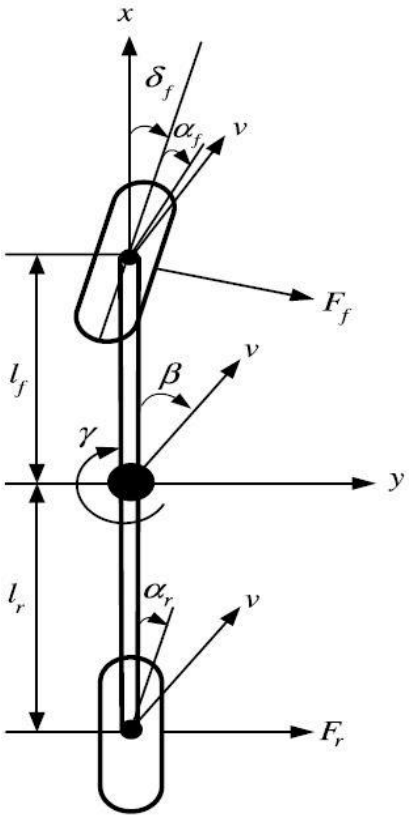

Figure 2.5: Simplified steady state handling model for a two axle vehicle (Keighobadi, 2014)

$$\delta f = \frac{L}{R} + \alpha_f - \alpha_r \quad (2.1)$$

$$= \frac{L}{R} + K_{us}\frac{a_y}{g} \quad (2.2)$$

This means that not the turning radius alone, but also the front tire slip angle and the rear tire slip angle also determine the steering angle required for negotiating a turn. K_{us} is the name for the understeer co-efficient.

2.1.9.3 *Understeer coefficient*

Depending on the understeer coefficient,K_{us}, values or the relationship between the slip angles for the front and rear tires, the steady-state handling behaviour is classified into three categories: neutral steer, understeer, and oversteer.

$$K_{us} = \frac{W_f}{C_{\propto f}} - \frac{W_r}{C_{\propto r}}$$

(2.3)

The under-steer coefficient's value fundamentally dictates how the vehicle behaves in a turn. If a vehicle deviates to the outside of a turn while maintaining a steady steer angle and increasing longitudinal speed, it is referred to be under-steer. The under-steer coefficient will have a magnitude greatr than zero (K_{us}>0) in the under-steer regime. At equal steer angle and forward speed, an oversteer vehicle will have its understeer coefficient less than zero (*Kus*<0) and tends to move towards the inner side of the turn. For a neutral steer vehicle having an understeer magnitude equals zero(*Kus*=0), the vehicle will remain completely on the turn path.

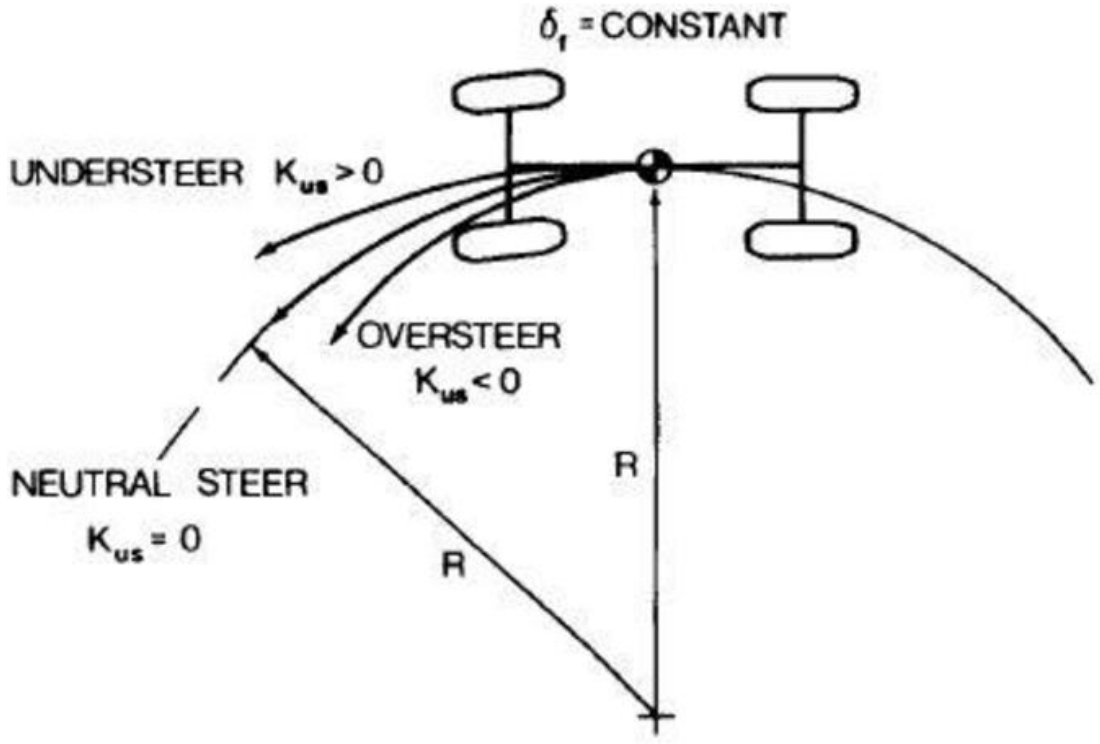

Figure 2.6: Curvature response of an understeer, neutral and over steer vehicle at constant steering angle (Wong, 2001)

In principle, when the understeer coefficient, K_{us}, is zero, tire slip angles for front and rear tire are the same ($\alpha_f=\alpha_r$, $W_f/C_{\alpha f} = W_r/C_{\alpha r}$, and $\delta_f = L/R$) (where, *L* is the wheelbase and *R* is the turn radius). In the under-steer region, K_us>0, and slip angle of the rear wheel is less than the slip

angle of the front wheel (i.e., $\alpha f > \alpha_r$, $W_f/C_{\alpha f} > W_r/C_\alpha$, and $\delta_f > L/R$). This means the turning radius will increase if the vehicle maintains the same steer angle while accelerating. In the over-steer regime, however, the turning radius gets smaller when the vehicle accelerates with an unvarying steer angle, (i.e., $\alpha_f < \alpha_r$, $W_f/C_{\alpha f} < W_r/C_\alpha$, and $\delta_f < L/R$). Generally, under-steer coefficient between the ranges of 2 to 6 deg/g is recommended for a good vehicle handling.

2.1.9.4 *Static margin*

Static margin is one of the parameter also used to measure the steady state handling behaviour of a vehicle. The point on the vehicle where a side force will not cause a steady state yaw velocity determines the SM., i.e. the neutral steer point (NSP). The NSP's position is determined by the total cornering force stiffness values at each vehicle end. The type of yaw reaction by the vehicle is determined by the position of the NSP in relation to the CG. The "static margin" is the distance between the CG and the NSP divided by the wheelbase. The vehicle is understeer if the static margin is at the rear of the CG and itis termed positive. At the CG the margin is zero and the vehicle is a neutral steer. If it is ahead of the CG the vehicle is oversteer.

2.1.9.5 *Yaw response*

When a vehicle negotiates a turn, the steer angle induced can be considered as input to the system (a vehicle can be considered as a system with various inputs). One of the motion variables regarded as an output from such a manoeuvre is the yaw velocity. It is a parameter used for comparing the responses from the steering of road vehicles. It is defined as the ratio of the steady-state yaw velocity to the steer angle. Under steady state conditions, the yaw velocity Ω_z is the ratio of the forward speed V to the turning radius R.

$$G_{yaw} = \frac{\Omega_z}{\delta_f} = \frac{V}{L + K_{us} + {V^2}/{g}} \tag{2.4}$$

With respect to the front wheel's steer angle, the above equation yields the yaw velocity gain. Controlling vehicle yaw rate is crucial to safety and is an important variable in vehicle dynamics control of road vehicles. Yaw stability control system among the typical systems for the control of lateral dynamics published in the literature (Aripin *et al*., 2014).

2. 2 Review of Past Work

2.2.1 Disabled tricycle

There are several studies on tricycle in the past. The ones relevant to this work are reviewed here.

Nag *et al.* (1982) found that cycling on a tricycle for 3 to 3.5 hours at a speed of 7.5 to 9.5 km/h allows an individual to cover roughly 30 km in a day. In terms of mechanical efficiency and cardio-respiratory response, studies have shown that arm-crank propulsion is superior to hand-rim propulsion (Muthuganapathy & Bandyopadhyay, 2011). However, during operations such as mounting and dismounting, riding, which involves sitting, pedalling, turning, and braking, an arm-crank driven trike must be ergonomically suitable and comfortable for the user.

Muthuganapathy and Bandyopadhyay (2011) worked on a trike with adjustable features. This was designed as a solution for mobility-challenged people with various needs due to stature, disability kind and severity, age or gender, and so on. Users choose a personalized design for a more pleasant experience. Users may select different seat heights, seat inclinations, back-rest angles, the placement of the crank at a certain spot, and the distance between the footrests. However, due to a variety of factors, including expense, it is not viable for every user to have a custom-made tricycle.

Holcomb *et al*. (2009) carried out research work on folding trike in Tanzania. They have cited works in Tanzania, Uganda and India that have shown preference for the tricycle over the wheelchair. The major limitations for the trike are poor manoeuvrability compared to the wheelchair especially in tight spaces, not suitable for indoor usage and too bulky for transportation. Their research effort was to develop a folding trike that will have the advantages

of both the standard manual trike and that of the wheelchair. They employed a standard wheelchair and designed an attachment to be retrofitted to convert the wheelchair into a trike.

Deans (2011) developed a wheelchair which can be converted to recumbent trike using advanced composite materials. The study investigates several devices available to users with disability and looks at the design of a modern, performance option with the aim to improve the usability of a tricycle by eliminating the need to leave the wheelchair to experience the attributes of a purpose built recumbent tricycle. The work also investigates manufacturing options for both workshop and commercial production.

Other designs employed the use of electric motor for propulsion. This will help in reducing the physical exertion from hand cranking thereby increasing travel range. However, their drawback is that the battery and the motor added to the weight. This concept shared similar problem with powered wheelchair because it becomes heavier, bulky and not easily transportable. It also shared similarities in power and transmission components like the powered wheelchair and has similar prospects technologically. It required to be charged often according to the designers/manufacturers efficiency and also on the quality of the parts used. Kalyani and Kirani (2014) worked on a power assisted tricycle in India. The Power Assisted Tricycle's design can be easily adapted to current hand-powered tricycles with minor changes. An electric motor, a driving system (transmission), and a power supply were included in the design (12 V Batteries). The power was transferred to the trike's rear wheels and the rated speed is 20 km/h.

Alimco, an Indian firm, makes electric trikes by simply substituting an electric drive motor for the hand crank system. The inherent problem of bulkiness and difficulty in transportation still remains. It can only be used outdoors and difficult to manoeuvre in tight spaces. Md Shahidul *et al*. (2012**)** worked on a solar powered tricycle in Bangladesh. Their design utilized an electric motor, solar panel charge controller, a 12V-80 AH battery to power the tricycle. The tricycle

is designed with a covered roof and weighs 85 Kg and load carrying capacity of 70 kg. The drawback of this design approach for the disabled is inability to be used indoors or in public buildings like classrooms, hospitals etc. therefore the user needs a wheelchair after alighting from the tricycle.

Hand tricycles have been developed for recreational sports and Paralympics. Jeang *et al*. (2015) developed a design for recreational sports for the disabled. The effort developed a workable design using quality function deployment methodologies (QFD) to capture customer requirements, seat design to adjust flexibly to fit different figures of disabled riders, light and compact structure using 6061 aluminium alloy tubes. Tests were performed based on ISO7176 standards. After road tests, recommendations were followed and electric assist drive was incorporated using hub brushless DC motor.

2.2.2 Rollover

Rollover is any manoeuvre of a vehicle to rotate 90 degrees or further about the X axis (longitudinal axis) till it makes contact with the ground. It is one of the dynamic manoeuvres that a vehicle may experience that can be life threatening to the occupants and has drawn a lot of research interest because of its severe consequence that may lead to death or injury. Consequently, a vehicle's low tendency to rollover during a turn or harsh manoeuvre is an important specification of a safe and comfortable vehicle.

In particular, rollover stability for three wheeled vehicles was investigated by Mukherjee *et al*. (2004). Licea *et al*. (2018) stated that though there have been initiatives to power small vehicles with electricity and diversify them, the active safety systems on motorcycles and tricycles (also known as auto rickshaws or Keke (NAPEP) were ignored until recently. For example, despite how vulnerable they are to rollover, electric tricycles (and even combustion engine tricycles) on the market today lack an active safety system for rollover risk prevention and mitigation. Licea *et al*. (2018), worked on a new rollover risk in delta type tricycles with a focus to

developing a new index for rollover and its mitigation through the development of a controller. Austin *et al*. (2015) described the determination of centre of gravity and dynamic stability of a tricycle used for cargo.

Hindering rollover improves the vehicle's lateral stability. This can be done by studying the specifications of the vehicle to get the best possible rollover threshold. Rollover may happen due to a combination of factors. Cross slope of roads and road disturbances like soft ground, curb impacts or other road disturbances may increase the lateral forces that may trip the vehicle. It can also happen on level and smooth road when the lateral accelerations surpass what the lateral weight shift on the tires can compensate. The lateral acceleration threshold, also known as the static stability factor (SSF), is dependent on the vehicles geometry. Rollover acceleration threshold for a four wheeled vehicle is given by:

$$a_y = \frac{bg}{2H} \quad (2.5)$$

Where *b* is the track width, *H* is the CG distance from the ground.

2.2.3 Tire camber

The commonly known ways to improve the stability in three wheel vehicles while turning and harsh manoeuvres is by cambering the wheels or tilting the body.Camber is the tilt of the wheel plane with respect to a plane perpendicular to the road surface as seen from the front and back of the vehicle. When the wheel inclination is outward relative to the body it is termed positive camber, when it goes inward relative to the body the camber is termed as negative.

Tateishi *et al*. (1986) investigated the effect of camber angle on controllability and stability of a vehicle using data from tire bench-test for simulation. The result showed that initial camber improves steering response and turning performance. By applying camber, cornering is shortened (Park *et al*., 2011)**.** It is important to constantly and accurately control camber angle to improve cornering, as it tends to affect the understeer characteristics of the vehicle

(Yoshinko *et al.*, 2014). This is achieved by the use of appropriate camber controllers (Woodruff *et al*., 2007)**.** A study by Mansour *et al*. (2019**)** showed that a proper strategy for camber control can improve both yaw rate and side-slip angle.

The camber thrust is one of the forces that balance the centrifugal force at the C.G. during steady-state cornering. Positive camber angles generate a camber thrust that acts in the same direction as centrifugal force. In this case, larger side-slip angles on the wheels are required to achieve steady-state cornering at the same radius and speed as when camber change is not taken into account. Negative camber angles, on the other hand, result in a camber thrust that acts in the opposite direction as the centrifugal force. The cornering force and wheel side-slip angles can be reduced in this situation (Abe, 2015).

Ataei *et al*. 2019 investigated the effects of cambering on overall vehicle stability, with a focus on applications to urban vehicles. To investigate the vehicle dynamics behaviour under cambering, a full vehicle model with a reliable tire model including camber effects is used. In addition, a linearised vehicle model is used to analyze the effects of camber lateral forces on vehicle dynamics. The vehicle behaviour is studied and compared for various camber angle configurations in the front and rear wheels. Then, to improve vehicle lateral stability, an active camber system is recommended. Performances of active front camber, active rear camber, and their combinations are specifically examined.

Edelmann *et al*. (2019) investigated the handling characteristics of a three-wheeled tilting vehicle. Vehicle models with varying levels of detail were developed to correspond to specific fields of investigation, and the proposed kinematics of the three-wheeler were assessed and optimized with respect to desired dynamic properties using a detailed multi-body system model. The partially unstable nature of the vehicle's motion suggests using an analytically derived, simplified model to focus on stability aspects and steady-state handling properties.

These investigations show the importance of using a steer-by-wire control system to assist the driver by stabilizing the vehicle's motion. As a result, an additional basic vehicle model was developed for control design, and an energy-efficient control strategy was presented. The dynamic properties of the optimized kinematics and control system were demonstrated by numerical simulation results, which were supported by successful prototype test runs.

Further advances in vehicle kinematic control technology are expected due to the rapid development of electric vehicles. As a result, it is believed that kinematic performance in the critical cornering range could be improved further by using electromagnetic actuators to control not only the steering angle but also the camber angle of the tires (Yoshino & Nozaki, 2014). Their study concentrated on a method of ground negative camber angle control that is proportional to the steering angle as a technique to improve manoeuvrability and stability to support the new era of electric vehicles. Camber angle control was discovered to control both the yaw moment and lateral acceleration at the turning limit in the critical cornering range. It was also confirmed that using actuators to implement ground negative camber angle control that is proportional to the steering angle improves both stability and steering effect in the critical cornering range. Implementing ground negative camber angle control that is proportional to the steering angle can result in dramatic improvements in cornering limit performance.

Tilting also improves the stability and manoeuvrability of a vehicle while negotiating a turn or in cornering. Tilting mechanisms are commonly used on narrow three-wheeled vehicles because of their usual stability issues due to small wheel track and the risk of their rollover (Vieira *et al.* 2007).

Generally, to evade instability of narrow vehicles with three wheels, it is essential to incorporate a tilting mechanism or wheel camber. The purpose of the vehicle determines the

choice of either a tilt or camber. In general, tilting system is suggested for manoeuvring and fast driving, where as for regular commuting in cities, camber system is better (Azadieh, 2014).

2.3 Research Gap

Investigations into the dynamic stability and control of light three-wheel vehicles are critical, particularly with the development of electric hub motors, which have allowed them to travel at much higher speeds. The WHO safety report on powered two and three wheelers expressed concern about this. Despite the fact that there is a large body of research on three wheelers, active safety systems on these vehicles were previously ignored (Licea *et al.*, 2018). The dynamic stability and control of larger three-wheel vehicles, such as auto rickshaws, were prioritized, while smaller vehicles, such as the disabled tricycle, were largely ignored. As the disabled tricycle's speed increases, it becomes increasingly important to investigate its stability and ways to improve it.

CHAPTER THREE

3.0 MATERIALS AND METHODS

3.1 Materials

Materials used in this work are listed in Table 3.1.

Table 3.1: Materials used for the tricycle

S/No	Description of Item	Quantity
1	Electric front drive hub motor 1000 W, 48 V	1
2	Controller 1000 W, 48 V	1
3	Speed LCD Display, 48 V	1
4	Brake disc and calliper	2
5	Throttle with reverse function	1
6	Brake lever	2
7	Linear String Encoder 24 VDC, CALT CESI-S1000P for steering angle measurement;	1
8	Indicator, HB961 for indicating the readings of steering angle; 24 VDC.	1
9	Shock Absorber, DNM 165	2
10	Tires 20 by 2.125, rated load of 70 kg each, maximum tire of pressure 60 psi	3
11	Standard bicycle front fork	
12	Lead acid Batteries, 12 V, 7.2 AH	4
13	20 mm stainless steel square tube	
14	25 mm stainless steel round tube	
15	30 mm stainless steel round tube	
16	40 mm stainless steel round tube	

Except for the electric bicycle kit (which includes items 1 through 6 in Table 3.1), the shock absorbers, and the linear string encoder with display, all of the materials used in this project were purchased locally. Because of its strength and light weight, stainless steel was chosen as the frame material. Instead of the typically utilized lithium-ion battery, the batteries were chosen due to their availability.

3.2 Methods

The design considerations in this work were focused on achieving optimum level of stability within the performance parameters of the tricycle.

3.2.1 Handling stability

The C.G location is an important vehicle property. Proper CG location promotes vehicle stability in terms of decreasing excessive yaw response, weaving at higher speeds, rollover resistance in curves and changes in road surfaces and swapping ends in braking owing to weight transfer.

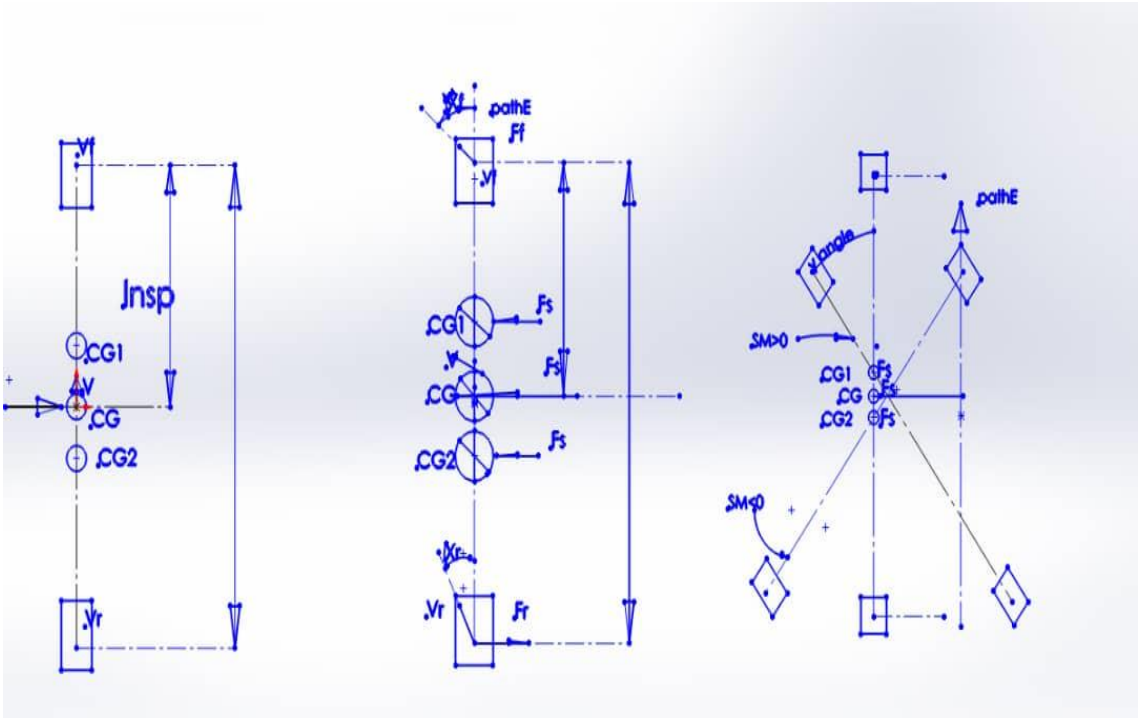

a **b** **c**

Figure 3.1: Bicycle model with side load (Starr, 2006)

In Figure 3.1, a four wheeled vehicle is represented as a bicycle model. The front and rear tires are represented as single at each end but are considered to have double the cornering stiffness of the dual tires at each axle of the four wheel vehicle. The model is shown in three conditions where it is assumed the CG is located on the centre line of the vehicle. The horizontal forces acting on the CG are of interest to this study. CG, CG1 and CG2 as labelled in Figure 3.1c are

the three considered positions of the CG. In Figure 3.1a, the vehicle is shown heading straight along path P with a steady velocity *V*. The axle lines above the front and rear tire contact patches have velocities V_F and V_R having same magnitude and direction as *V*.

In Figures 3.1b and 3.1c, side load F_S is applied at each centre of mass and the ensuing responses are shown, giving that there are no steering corrections from the driver makes. The vehicle is illustrated in Figure 3.1b travelling along path P at the time of the side load application. To offset the side load, lateral forces at the tires, designated as F_F and F_R, would develop. This would result to presence of slip angles $\propto_F$ and $\propto_R$as the velocities deviate from their initial paths. Figure 3.1C depicts three vehicle reactions shortly after a side force is applied, with slip angles and tire forces eliminated for clarity. The yaw reaction is a sideways displacement of the CG away from path P and an angular rotation about the CG, which is denoted by angle θ. A point where a side force can be applied without the corresponding yaw response is known as the "Neutral Steer Point" (NSP). The NSP's placement is determined by the overall cornering stiffness values at each vehicle end. The distance between the front axle line and the NSP is calculated as follows:

$$LNSP = \left[\frac{\bar{C}_R}{\bar{C}_F + \bar{C}_R}\right] L$$

(3.1)

Where:C_F,C_R are cornering stiffness values of a single front and rear tire, N/deg.

$\bar{C}_F$, $\bar{C}_R$ are total cornering stiffness values for the four wheel bicycle model:

$\bar{C}_F$, = $2C_F$

$\bar{C}_R$, = $2\ C_R$

L = wheel base

l1 = distance between front axle line and the CG, m.

The type of yaw reaction by the vehicle is determined by the position of the NSP in relation to the CG. The “static margin” (SM) is given by the quotient of the wheel base and the distance between the CG and the NSP.

$$SM = \left[\frac{\bar{C}_R}{\bar{C}_F + \bar{C}_R} - \frac{l_1}{L}\right]$$

(3.2)

Static margin is a measure of the vehicle's yaw reaction and its value can be positive, negative, or zero, and. Consider a scenario in which the front axle's centre of mass is around a half of the wheelbase away from the front axle and the same tire types are utilized on both ends. In that case, $\bar{C}_F = \bar{C}_R$and equation 3.2 can be rewritten as:

$$SM = \left[\frac{1}{2} - \frac{l_1}{L}\right]$$

(3.3)

From equation 3.3 above indicated that when the CG is located at half the wheelbase,$l_1 = \frac{L}{2}$, then $SM = 0$. In a situation like this, a load at the *CG* will not yield a yaw response. As shown in Figure 3.1 c, both tires slip angles are equal and the vehicle will side slip. This is referred to as neutral steer, and it is assumed stable.

SM is positive (SM = +) when $\frac{l_1}{L}$ is smaller than half of the wheelbase, when the *CG* is located in front of the NSP shown as *CG1* in Figure 3.1 c. The yaw response is illustrated in the Figure. The vehicle continues in the path of the applied force because the rear slip angle is smaller than the front slip angle. This is a desirable condition known as understeer.

When the location of the *CG* is at the back of the *NSP*, then $\frac{l_1}{L}$ is larger than half the wheelbase, the *SM* is considered negative (*SM*= -). The yaw response is illustrated in Figure 3.1 c, when the rear slip angle is greater than that of the front, the vehicle travels in a direction contrary to the applied force. This situation is termed as oversteer and is regarded as unstable.

As indicated above, SM values of zero or positive are preferable for stability.

3.2.1.1 *Vehicle response in a turn*

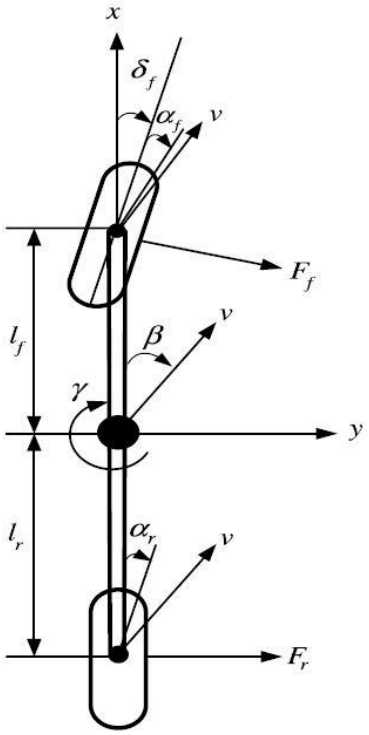

Figure 3.2: Simplified steady state handling model for a two axle vehicle (Keighobadi, 2014)

Tires create lateral force and experience lateral slip during cornering. Newton's second law, as well as the equations describing the vehicle geometry in a turn, are used to obtain the steady state cornering equations. The lateral force, F_y, is called the cornering force.

$F_y = C \propto$
(3.4)

Where:

C = cornering stiffness

α = Slip angle

Consider a vehicle moving forward at speed, V; the sum of lateral forces at the tires must equal mass times centripetal acceleration.

$$\sum F_{y=} F_y f + F_y r = {MV^2}/{R}$$

(3.5)

Where:

F_{yf} = Lateral cornering force at the front axle,

F_{yr} = Lateral cornering force at the rear axle

M = Vehicle mass

R = Radius of turn

V = Forward velocity

The front and rear lateral forces must sum up to zero for the vehicle to be in moment equilibrium around its CG.

$$F_{yf} b - F_{yr} c = 0$$

(3.6)

$$F_{yf} = \frac{F_{yr} c}{b}$$

$${MV^2}/{R} = F_{yr}\left(\frac{c}{b} + 1\right) = {F_{yr}\,(b + c)}/{b} = F_{yr}\frac{L}{b}$$

$$F_{yr} = \frac{Mb}{L}\left(\frac{V^2}{R}\right)$$

(3.7)

The mass on the rear axle, *Mb/L*, is expressed by the term W_r/g. Wr/g times the lateral acceleration at that time equals the lateral force exerted at the rear axle as shown above in Equation 3.7. Similarly, solving for F_{yf} indicates that W_f/g multiplied by the lateral acceleration at that moment in time is the lateral force at the front axle.

Since the lateral forces are known, both front and rear slip angles, from equation 3.4 becomes,

$$\propto_f = W_f \, V^2 \Big/ (C_f g R)$$

(3.8)

$$\propto_r = W_f \, V^2 \Big/ (C_r g R)$$

(3.9)

It was established from the geometry of Figure 3.2 that the steering angle, δ, is

$$\delta = 57.3 \, \frac{L}{R} + \propto_F - \propto_R$$

(3.10)

Substituting equations 3.9 and 3.10

$$\delta = 57.3 \, \frac{L}{R}\left[\frac{W_F}{C_F} + \frac{W_R}{C_R}\right]\frac{V^2}{gR}$$

(3.11)

The expression$V^2/gR$is called the lateral acceleration expressed in fraction of *g*'s, and is expressed as:

$$a_y = {V^2}/{gR}$$

(3.12)

Where;

V = velocity of CG along the path, *m/s*,

R = radius of CG path, *m*,

g = acceleration due to gravity, m/s^2

The expression in bracket is referred to as the "understeer gradient", *K*, is significant in this study.

$$K = \left[\frac{W_F}{C_F} - \frac{W_R}{C_R}\right],$$

(3.13)

Where:

W_f = weight on front tires, N.

W_r = weight on rear tires, N.

C_f = total cornering stiffness for front tires, N/deg

C_r = total cornering stiffness for rear tires, N/deg

Equation 3.11 can be written as:

$$\delta = 57.3\frac{L}{R} + (K)(a_y)$$

(3.14)

By combining equations 3.3 and 3.6, the steering angle can be expressed in terms of the static margin, to yield:

$$\delta = 57.3\frac{L}{R} + (W)\left[\frac{\bar{C}_F+\bar{C}_R}{\bar{C}_F\bar{C}_R}\right](SM)(a_y)$$

(3.15)

It is very significant how steering angle changes as lateral acceleration, ay, increases when analyzing stability in a turn. Each of the above expressions for steering angle is the sum of a constant term and any of the following terms, which might become positive, zero, or negative.

From Equation 3.10, we have (αf-αr)

From equations 3.13 and 3.14 $K = \left[\frac{W_F}{C_F} - \frac{W_R}{C_R}\right]$

From equation 3.2 and 3.15 $SM = \left[\frac{\bar{C}_R}{\bar{C}_R+\bar{C}_F} - \frac{l_1}{L}\right]$

The conditions that cause these terms' signs to change are the same: for instance, when $\alpha_f > \alpha_r$, *then K>0 and SM>0*. The sign change for these expressions determines the vehicle's stability and also defines its steering characteristics.

Neutral Steer: $\alpha_f = \alpha_r$, *K=0, SM=0*

From equation 3.14, when K=0 then steering angle, δ does not change from the value *57.3 L/R.* Higher lateral force would be needed at both vehicle ends if it was in a path of circular of radius *R* and gradually increasing the velocity, causing a_y to increase. This would necessitate slip angles α_f *and* α_r to increase. The vehicle rotates slightly relative to the direction of velocity *V* for a neutral steer vehicle, causing a decrease in the side slip angle β (which may possibly become negative) and consequently increasing both front and rear slip angles by an equal amount while δ remains the same.

Understeer: *αf>αr, K>0, SM>0*

Because the front slip angle is greater than the rear, the required steering angle increases with speed. It does, however, self-correct. If the driver fails to increase δ, the positive yaw will make the front end of the vehicle to deviate away from the initial path, making the radius *R* larger and decreasing the centrifugal force. As a result, a positive SM is referred to as "stable".

Oversteer: *αr>αf, K<0, SM<0*

Because the rear slip angle is greater than the front, the required steering angle becomes smaller than its neutral steer value. That is, the back of the vehicle is sliding to the side more than the front. If the driver does not perform a correction, the vehicle's rear drifts outward from its initial route, reducing the radius, *R*, and increasing the centrifugal force, necessitating a larger adjustment. The correction is the well-known "turn in the direction of the skid" and if not done early enough, the vehicle will spin. Thus a negative *SM* is termed "unstable".

3.2.1.2 *Applications to three wheeled vehicle with a delta configuration*

The configuration for a delta tricycle will have its rear wheels on the same axle line and having the same distance from the fore aft vehicle centre line while the front wheel is placed at the centre line. Steering is provided by the front wheel. For the expressions of *SM* and *K* accordingly Equations 3.2 and 3.13 were adjusted, but *the K≥0 and SM≥0* condition to achieve stability does not change. The cornering stiffness values are the expressions that must be changes. The front wheel cornering stiffness $\bar{C}_F$ value remains single while that of the rear tire denoted as $\bar{C}_R$ will be doubled.The expressions for *K* and *SM* then become:

$$K = \left[\frac{W_F}{C_F} - \frac{W_R}{\bar{C}_R}\right]$$

(3.16)

$$SM = \left[\frac{\bar{C}_R}{C_F + \bar{c}_R} - \frac{l_1}{L}\right]$$

(3.17)

The threshold values of $K = 0$ and $SM = 0$ can be attained if the tires on all the wheels are identical and having equal weight distribution as well. The cornering stiffness of the tires will be the same, and the weight distribution will be:

$$W_F = \frac{W}{3}$$

(3.18)

$$W_R = \frac{2W}{3}$$

(3.19)

$$l_1 = \frac{2L}{3}$$

(3.20)

The cornering stiffness values in the expression for K are assumed to be constant for slip angles that are small for a specified load. Since lateral force increases as a_y increases, the relationship between lateral force versus slip angle moves past the linear range. There will be lateral transfer of weight from the inner tires to the outer ones; however, the summed up value for the cornering stiffness of the two rear tires will be smaller than the sum of their statically loaded values due to load sensitivity.

For a tricycle with a delta layout, lateral weight transfer has substantial design implications. The rear wheels will experience lateral load transfer, lowering the $\bar{C}_R$ value due to load sensitivity. It can be shown from Equation 3.16 that this will result in a negative K value. Rear wheel camber will be introduced to raise the value of $\bar{C}_R$.

3.2.1.3 *Wheel camber consideration*

A given tire's cornering force and alignment moment are non-linear functions of the slip angle and vertical load. The lateral force created at the contact patch, called the camber thrust $F_y\gamma$, is affected by wheel camber. Camber stiffness data for the 20 by 2.125 bicycle tire is not available. Four distinct camber angles 0º, 5º, 10º and 15º were used. Excessive camber angle affects tire wear, therefore limiting it to 15º is necessary.

3.2.2 Design consideration for rollover stability

Kinematic model of a three wheel vehicle is shown Figure 3.3

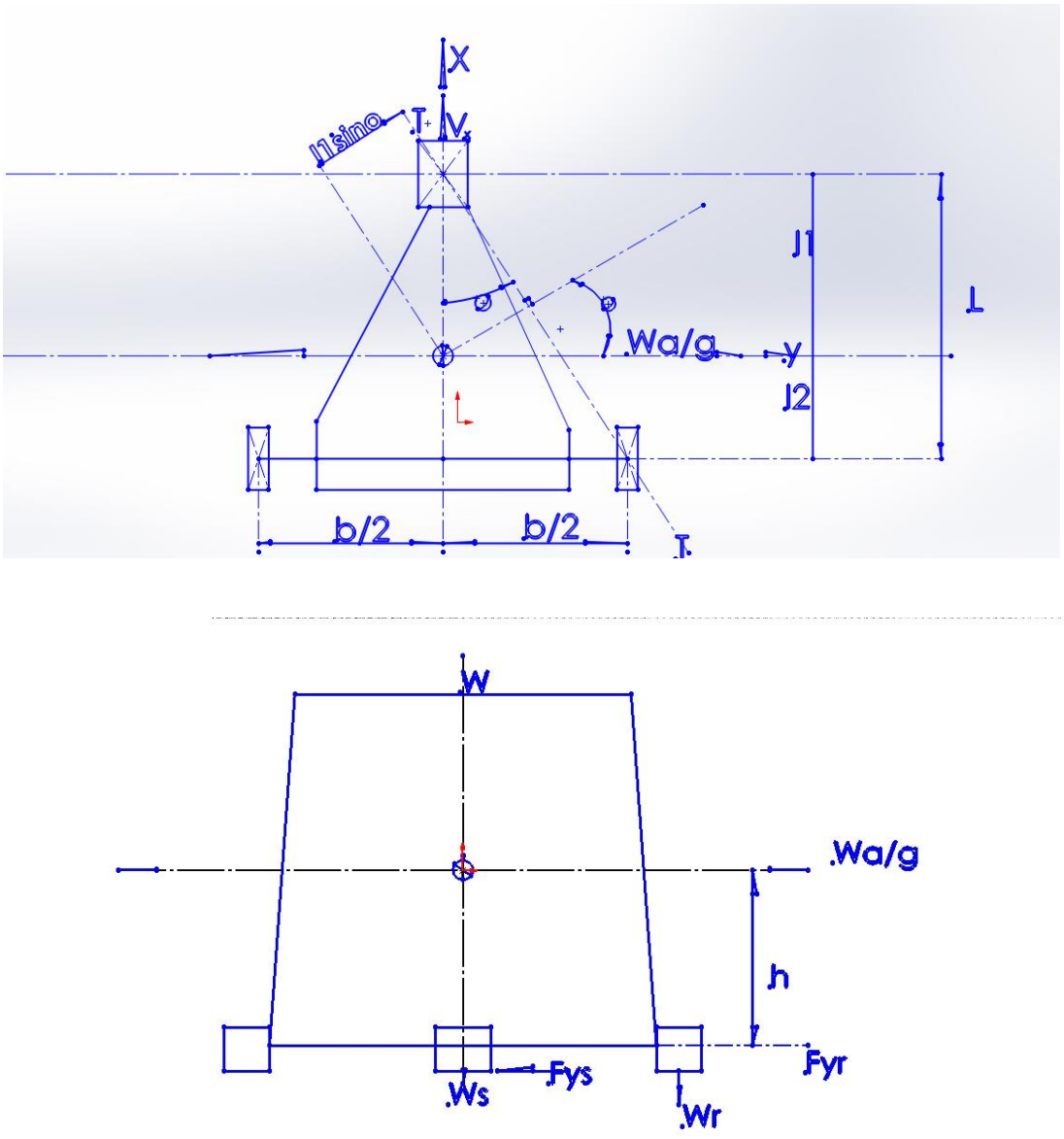

Figure 3.3: Lateral acceleration, three wheeled vehicle with two wheels on the rear axle, top and rear view (Huston *et al*.,1982)

Resistance to rollover is a good indication of vehicle stability. Three wheelers are considered stiff in roll (Van Valkenburgh, 1982)**.** The value of lateral acceleration, a_y, required for the inside tires to experience zero vertical loads was determined using a quasi-static rollover model. That maximum amount of lateral acceleration is termed as the rollover threshold. The longitudinal positioning of the CG, its height and the vehicle wheel track, are all factors in determining the value for a three-wheeler.

Lateral acceleration acts perpendicular to the centreline of the vehicle. From Figure 3.3, the TT axis represents the tipping axis. To resist rollover, there must exit a negative clockwise moment about the TT axis, if viewed from the vehicle's rear.

Summing moments about the tipping axis, TT, gives:

$$\sum M_{TT} = -Wl_2 sin\theta + \frac{W}{g} ahcos\theta < 0$$

(3.21)

The relationship can be re-written

$$\frac{a}{g} < \frac{l_2}{h} tan\theta$$

(3.22)

Since θ is a function of the vehicle geometry; it can be shown that:

$$tan\theta = \frac{b}{2L}$$

(3.23)

Substituting equation 3.23 into 3.22 yields:

$$\frac{a}{g} < \frac{b}{2h}\frac{l_1}{L} = F_c$$

(3.24)

Equation 3.24 above is the requisite condition to prevent rollover.

A vehicle's lateral acceleration while in a turn of radius *R* can be written in terms of the turning radius and forward speed *V*.

$$a = \frac{V^2}{R}$$

(3.25)

The rollover speed can be obtained by substituting equation 3.22 into 3.24.

$$V_{ro} = \sqrt{\frac{gRbl_1}{2hL}}$$

(3.26)

3.2.2.1 *Rollover stability during lateral acceleration in a turn*

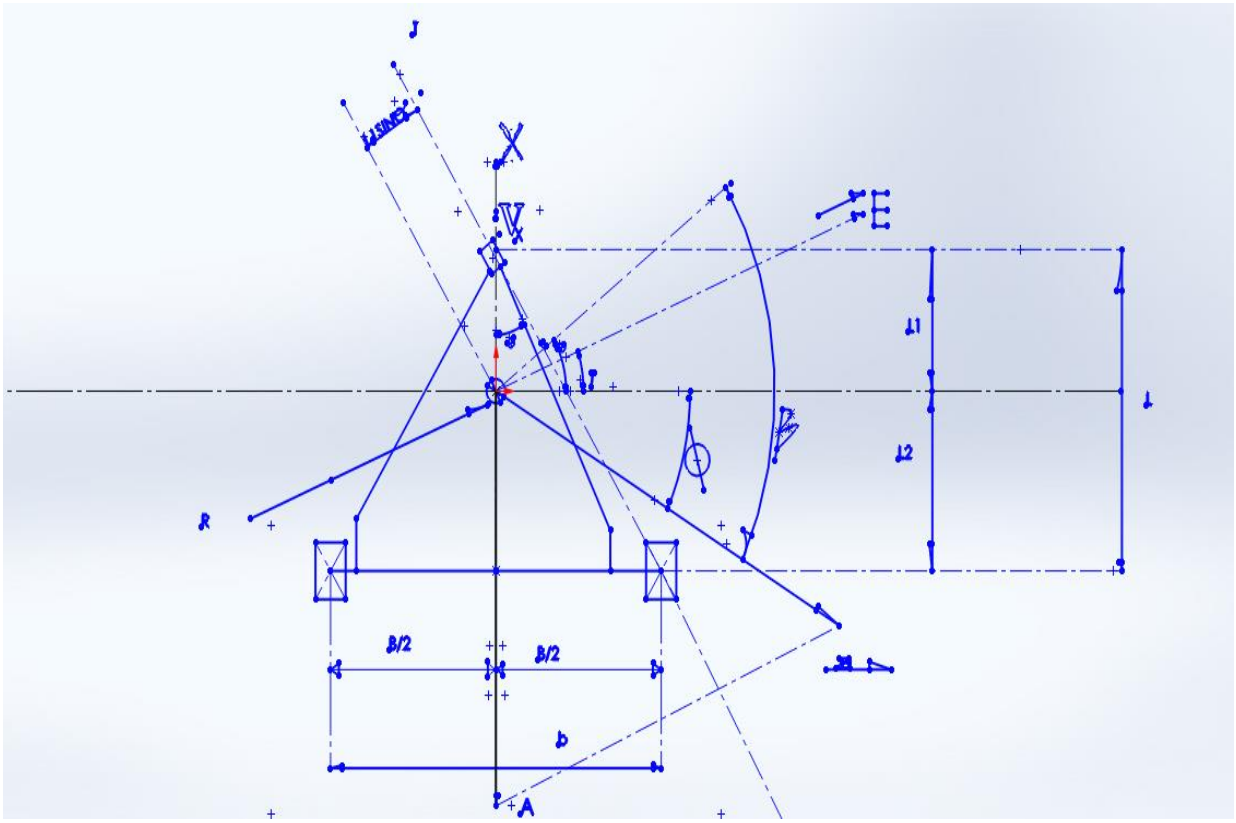

Figure 3.4: Lateral acceleration, three wheeled vehicle accelerating in a turn (Huston *et al.*,1982)

Consider the rollover stability when accelerating a turn. Figure 4 depicts a three wheel vehicle model while accelerating in a turn An inertia vector, symbolized by the letter A, will result from the longitudinal acceleration. The lateral acceleration caused by the steady state turn will result in an inertia vector symbolized by the letter E. The resultant vector of A and E is denoted by the sign Z.

The magnitudes of the inertia force vectors A and E are as follows:

$$A = \left|\vec{A}\right| = \frac{W}{g}a$$

(3.27)

And

$$E = \left|\vec{E}\right| = \frac{W}{g}\frac{V^2}{R}$$

(3.28)

The resultant expression for the inertia force vector,$\left|\vec{Z}\right|$, is:

$$\vec{Z} = \left|\vec{Z}\right| = [A^2 + E^2 - 2AEsin\gamma]^{\frac{1}{2}}$$

(3.29)

$$\emptyset = tan^{-1}\frac{Esin\gamma - A}{Ecos\gamma}$$

(3.30)

$$\theta = tan^{-1}\left(\frac{b}{2L}\right)$$

(3.31)

Where:

W = total vehicle weight

g= gravitational acceleration

a=longitudinal acceleration

V= Vehicle's forward speed

R= Turn radius

Angles γ, ϕ, α, β are:

γ = angle between line drawn from the centre of curvature to the vehicle's centre of mass and the line drawn from the centre of curvature to the vehicle's rear axle.

θ = angle between the centre line of the vehicle to the tipping axis, TT.

Φ = angle between resultant vector Z and the x axis.

β = angle between resultant vector Z and the line drawn perpendicular to the tipping axis through the mass centre of the tricycle and the rear wheels.

To guarantee rollover stability in a turn while accelerating, the clockwise moment about the axis of tipping, axis TT, has to be negative. The three-wheeled vehicle with a delta layout's rollover stability equation is as follows:

$$Z\cos\beta < \frac{Wb}{2h}\frac{l_1}{\left[L^2+\left(\frac{b}{2}\right)^2\right]^{\frac{1}{2}}}$$

(3.32)

Where $\beta = \emptyset + \theta$

(3.33)

3.2.2.2 *Rollover stability while braking in a turn*

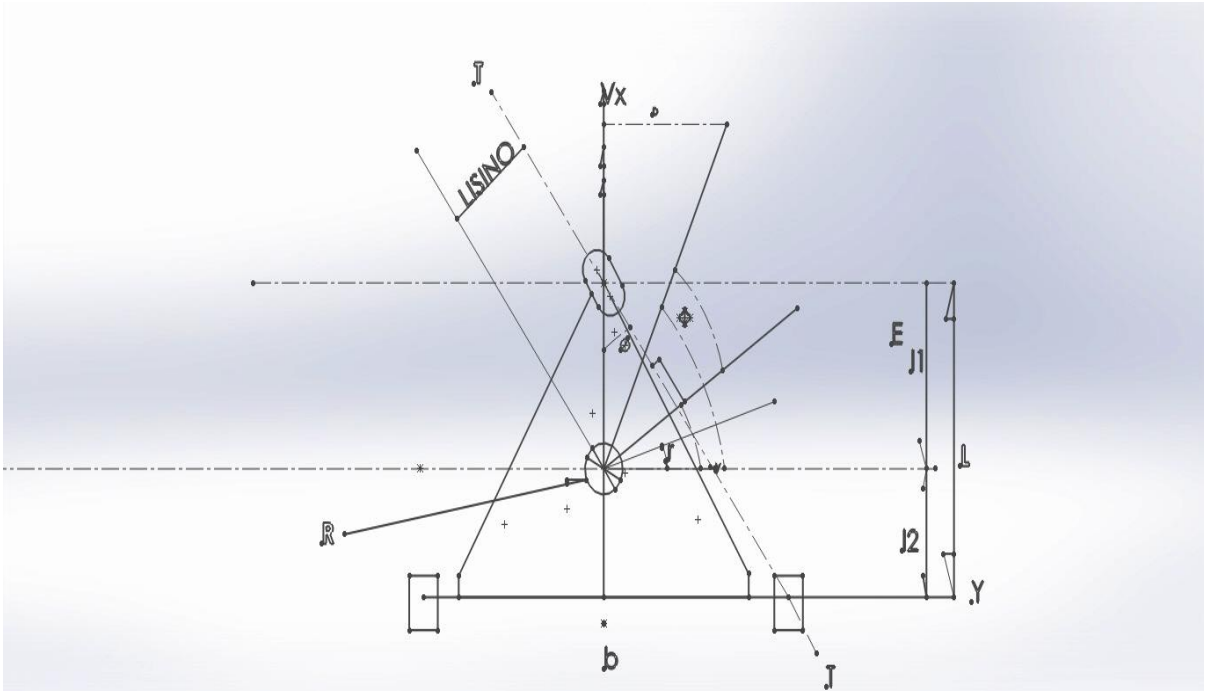

Figure 3.5: Lateral acceleration, three wheeled vehicle braking in a turn (Huston *et al.*,1982)

All symbols are as represented in Figure 3.4; the inertia force vector as a result of braking is represented by symbol *D* in Figure 3.5. The magnitude of the vector is expressed as:

$$D = \left|\vec{D}\right| = \frac{W}{g}d$$

(3.34)

The rollover stability equation during braking in a turn is expressed as equation 3.32:

$$Zcos\beta < \frac{Wb}{2h}\frac{l_1}{\left[L^2+\left(\frac{b}{2}\right)^2\right]^{\frac{1}{2}}}$$

Where $\beta = \phi - \theta$

(3.35)

The inertia acceleration force, *A*, in equations 3.29 and 3.30 should be replaced by the negative of the inertia force, *D*, when braking in a turn to get the resulting vector *Z* and its orientation angle, ϕ.

3.2.3 Testing of handling characteristics

It is required that tests are performed to measure the steady state handling behaviour of the tricycle and the rollover stability.

3.2.3.1 *Constant radius test*

The understeer gradient, which is a steady state attribute and a measure of any vehicle's handling behaviour, was verified using the constant radius test. The experimental method is based on equation 3.14: $\delta = 57.3\frac{L}{R} + K(a_y)$

The Constant Radius Test is performed by driving in a circle of radius, *R*, with a constant velocity, *V*, while measuring the steering angle. The speed is gradually increased and the measurements repeated until the vehicle reaches a specified maximum lateral acceleration, a_y, or is unable to continue on its course. The value at which the maximum lateral acceleration, $a_{y,}$ value occurs corresponds to the "tipping threshold". The values for the velocity were gotten from the speed display of the tricycle. The steering angle, δ, was measured with a rotary string encoder, and the results were shown on the indicator. The steering angular displacement was used to calibrate the linear displacement of the rotary string encoder. The lateral acceleration, a_y values were computed from equation 3.12.

The slope of the steer angle-lateral acceleration curve can be used to establish the handling behaviour of the vehicle. From Equation 3.14, for a constant turning radius, the slope of the curve is given by

$$\frac{d\delta_f}{d\left({}^{a_y}/_{g}\right)} = K \tag{3.36}$$

This means that the understeer coefficient's value is represented by the curve's slope. The vehicle is neutral steer if the steer angle necessary to maintain a constant radius turn is the same at all forward speeds (i.e., the slope of the steer angle-lateral acceleration curve is zero). When the slope of the steer angle-lateral acceleration curve is positive, the vehicle is said to be understeer, indicating that the understeer coefficient K is larger than zero. When the slope of the curve is negative, the vehicle is said to be oversteer, indicating that the understeer coefficient K is less than zero. The obtained K value can be employed to get thevehicle motion variables like yaw velocity response, lateral acceleration response and curvature response, which are considered outputs to the driver's steering inputs. Yaw velocity Ω_z, of the vehicle under steady-state conditions is the ratio of the forward speed V to the turning radius R. The yaw velocity response is defined as the ratio of the steady-state yaw velocity to the steer angle given by:

$$G_{yaw} = \frac{\Omega_z}{\delta} = \frac{V}{L + K{}^{V^2}/_{g}} \tag{3.37}$$

Lateral acceleration gain, G_{acc}, defined as the ratio of the steady-state lateral acceleration to the steer angle, is a common parameter used for evaluating the vehicle's steering response. It is given as:

$$G_{acc} = \frac{{V^2}/{gR}}{\delta} = \frac{\left({a_y}/{g}\right)}{\delta} = \frac{V^2}{gL+KV^2}$$

(3.38)

The ratio of the steady-state curvature 1/R to the steer angle is one of the parameters usually used for evaluating the characteristics of the vehicle's response. This parameter is expressed by:

$$\frac{{1}/{R}}{\delta} = \frac{1}{L+k{v^2}/{G}}$$

(3.39)

3.2.3.2 *Rollover threshold test*

Rollover threshold tests were carried out to establish the actual velocity at which rollover occurs. The test was performed in a flat paved surface area with full circles of 5 m, 10 m and 15 m radii and semi circles of 20 m, 25 m and 30 m radii because of insufficient space. The tricycle was driven at varied camber angles for each radius and the speeds were recorded at which attempt to rollover was observed.

3.3 Design Calculations

The geometric parameters of the tricycle were considered to achieve optimum performance within its operational limitations.

Design parameters used are listed on the Table 3.2

Table 3.2: Design Parameters

Parameter	Description	Value
L(m)	Wheel base of vehicle	1.2 m
$l_1(m)$	Length, from C.G to front axle	0.65 m
l2(m)	Length, from CG rearward to the rear axle	0.55 m
b(m)	Wheel track of vehicle	0.64 m
W(kg)	Weight, vehicle and rider	120 kg
h(m)	Height, CG from the ground	0.55 m
δ *(Deg)*	Steering angle	3^o
R(m)	Radius of turn	30 m
V(m/s)	Velocity	8.33 m/s
$g(m/s^2)$	Acceleration of gravity	9.82 m/s^2
$a(m/s^2)$	Acceleration, longitudinal	6.5 m/s^2
$d(m/s^2)$	deceleration (the braking requirement for a bicycle is that it must come to complete stop from a speed of 25 km/h within 4.57 m, according to the United States Consumer product Safety Commission.)	-5.27 m/s^2

3.3.1 Calculation for rollover stability

Condition for rollover stability from Equation 3.24 is given by

$$\frac{a_y}{g} < \frac{b}{2h}\frac{l_1}{L}$$

$$a_y = \frac{V^2}{R}$$

$$a_y = \frac{8.33^2}{30} = 2.31\ {}^{m}/_{s^2}$$

Therefore;

$$\frac{2.31}{9.82} < \frac{0.64}{2 * 0.55}\frac{0.65}{1.2}$$

$$0.2352 < 0.315$$

From the above solution to conditions for rollover stability, it can be seen that the conditions for rollover stability has been achieved for the selected parameters.

3.3.2 Rollover velocity

The speed at which rollover occurs can be calculated from equation 3.25

$$V_{ro} = \sqrt{\frac{gRbl_1}{2hL}}$$

$$V_{ro} = \sqrt{\frac{9.82 * 30 * .64 * .65}{2 * .55 * 1.2}}$$

$V_{ro} = 9.64\ {}^{m}/_{s}$ (34.70 km/h)

From the above solution it can be seen that rollover will occur at 34.70 km/h.

3.3.3 Rollover stability during lateral acceleration in a turn

The condition for rollover stability while accelerating in a turn is given by the condition in Equation 3.32,

$$Z\,cos\beta \; < \frac{Wb}{2h} \frac{l_1}{\left[L^2 + \left(\frac{b}{2}\right)^2\right]^{\frac{1}{2}}}$$

Where Z, from Equation 3.29, is

$$\vec{Z} = \left|\vec{Z}\right| = [A^2 + E^2 - 2AEsin\gamma]^{\frac{1}{2}}$$

A and E, from Equations 3.27 and 3.28 respectively, are given as,

$$A = \left|\vec{A}\right| = \frac{W}{g}a$$

$$E = \left|\vec{E}\right| = \frac{W}{g}\frac{V^2}{R}$$

The angle β is given by

$$\beta = \; \emptyset + \theta$$

While the angles ϕ and θ, from Equations 3.30 and 3.31 respectively, are given as

$$\emptyset = tan^{-1}\frac{Esin\gamma - A}{Ecos\gamma}$$

$$\theta = tan^{-1}\left(\frac{b}{2L}\right)$$

The angle γ from the geometry of the turning radius, as depicted in Figure 3.6, can be seen to be the same as the steering angle δ.

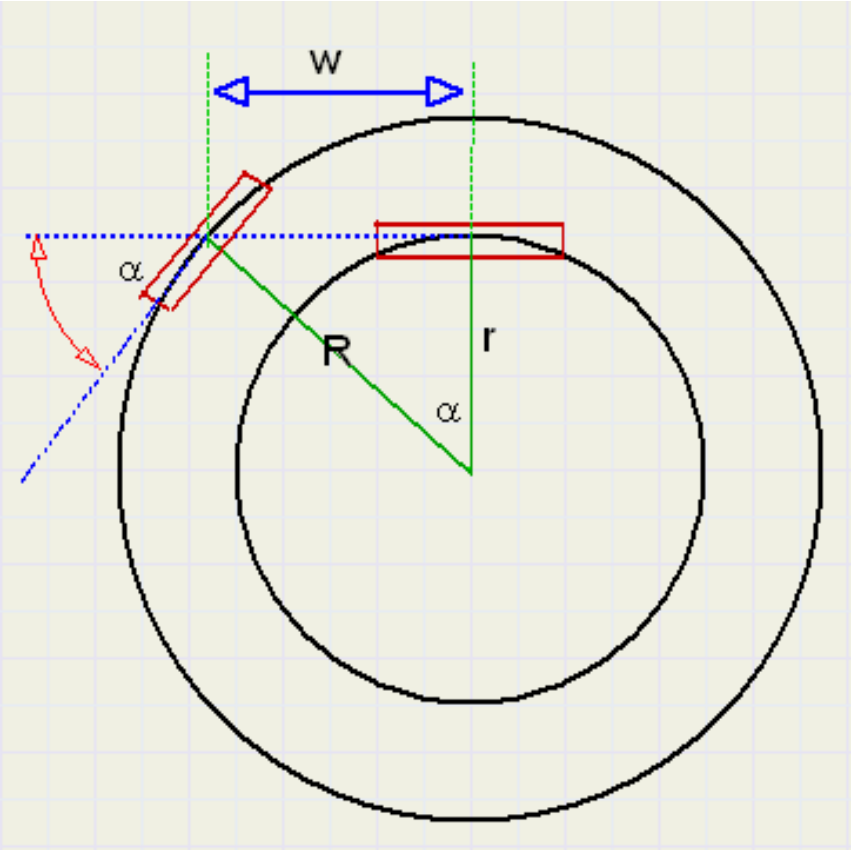

Figure 3.6: Steering angle, $\boldsymbol{\delta}$ (www.davdata.nl)

$\gamma = \delta = 3^o$

Therefore,

$$A = \left|\vec{A}\right| = \frac{120}{9.82}6.5 = 79.43$$

$$E = \left|\vec{E}\right| = \frac{120}{9.82}\frac{8.33^2}{30} = 28.26$$

$$\vec{Z} = \left|\vec{Z}\right| = [79.43^2 + 28.26^2 - 2 * 79.43 * 28.26sin3]^{\frac{1}{2}} = 82.90$$

$$\emptyset = tan^{-1}\frac{28.26sin3 - 79.43}{28.26cos3} = -2.76°$$

$$\theta = tan^{-1}\left(\frac{.64}{2 * 1.2}\right) = 14.93°$$

$$\beta = -2.76 + 14.93 = 12.17°$$

Therefore the equation for the condition for rollover stability while accelerating in a turn can be resolved

$$82.90\cos(12.17) < \frac{120 * 0.64}{2 * 0.55}\frac{0.65}{\left[1.2^2 + \left(\frac{0.64}{2}\right)^2\right]^{\frac{1}{2}}}$$

$$81.04 < 36.54$$

It can be seen from the above solution that the condition could not be fulfilled.

3.3.4 Rollover stability while braking in a turn

$$Z cos\beta < \frac{Wb}{2h}\frac{l_1}{\left[L^2 + \left(\frac{b}{2}\right)^2\right]^{\frac{1}{2}}}$$

Where β = ϕ - θ

$$D = \left|\vec{D}\right| = \frac{W}{g}d$$

$$E = \left|\vec{E}\right| = \frac{W}{g}\frac{V^2}{R}$$

$$\vec{Z} = \left|\vec{Z}\right| = [D^2 + E^2 - 2DEsin\gamma]^{\frac{1}{2}}$$

$$\emptyset = tan^{-1}\frac{Esin\gamma - D}{Ecos\gamma}$$

$$\theta = tan^{-1}\left(\frac{b}{2L}\right)$$

Solving for the resultant, D,

$$D = \left|\vec{D}\right| = \frac{120}{9.82}(-5.27) = -64.40$$

$$E = \left|\vec{E}\right| = \frac{120}{9.82}\frac{8.33^2}{30} = 28.26$$

$$\vec{Z} = \left|\vec{Z}\right| = [-64.40^2 + 28.26^2 - 2 * (-64.40) * 28.26sin3]^{\frac{1}{2}} = 103.17$$

$$\emptyset = tan^{-1}\frac{28.26sin3 + 97.76}{28.26cos3} = 3.52°$$

$$\theta = tan^{-1}\left(\frac{.64}{2 * 1.2}\right) = 14.93°$$

$$\beta = 3.52 - 14.93 = -11.41°$$

Therefore the equation for the condition for rollover stability while braking in a turn can be resolved.

$$103.17\cos(-11.41) < \frac{120 * .64}{2 * 0.45}\frac{.65}{\left[1.2^2 + \left(\frac{0.64}{2}\right)^2\right]^{\frac{1}{2}}}$$

$$101.13 < 36.54$$

It can be seen from the above solution the condition could not be fulfilled.

The camber impact on the tricycle wheel is not taken into account in the analytical calculations.

3.4 Determination of Centre of Gravity and Weight Transfer in Motion

The tilting method was used for the CG height. The tricycle was placed parallel to the tilting axis (X). The wheels were supported. The tilting was done very slowly until the tricycle was no longer in a stable position and falls to the ground. The angle of the unstable position was measured. Three measurements were taken independently, and the height of CG was calculated using the average of the three tilting angles. Tilting tests were conducted in both directions, yielding two tilting angles: left and right.

The critical angle was established to be 30^{o}. The CG height was calculated using the formula:

$$h = {}^{0.5\ b}/_{\tan 30}$$

(3.40)

Where b is the wheel track of the tricycle given as 0.64m

$$h = {}^{0.5 * 0.64}/_{\tan 30}$$

h = 0.55m

The CG height above the ground is established to be 0.55m.

Plate VIII: CG Height test, June, 2021

The CG's longitudinal location was established by measuring the front axle weight and the rear axle weight of the tricycle on a level surface. Load cells were used as seen in the picture below.

Plate IX: Axle weight measurement, July, 2021

Plate X: Tricycle weight measurement, July, 2021

$$\sum F_Y = 0$$

$$W - (R_f + R_r) = 0$$

$$W = (R_f + R_r)$$

(3.41)

$$\sum M_a = 0$$

$$R_f L - W l_2 = 0$$

(3.42)

$$l_2 = L\left({}^{R_f}/_{W}\right)$$

But $W_f = R_f$ *and* $Wr = R_r$

Wf =23.6 kg, Wr=26 kg

W=49.6 kg

$$l_2 = 1.2\left({}^{23.6 * 9.81}/_{49.6 * 9.81}\right)$$

l_2= 0.52 m

The CG is located 0.52 m from the rear of the tricycle with no rider on it.

With a rider on the tricycle the front and rear weight distribution were measured as follows:

W_f *= 57.6 kg, Wr = 68 kg*

l_2 was calculated to be 0.55 m.

There is a slight forward shift of the CG by 30 cm

3.4.1 Weight distribution during acceleration

During acceleration on level ground, weight transfer occurs from the front axle to the rear axle.

This is calculated from equation 3.42.

$$W_f = W\left(\frac{l_2}{L} - \frac{a}{g}\frac{h}{L}\right)$$

(3.43)

$$W_f = 125.6\left(\frac{0.55}{1.2} - \frac{6.5}{9.81}\frac{0.55}{1.2}\right)$$

$$W_f = 19.4\ 2\text{kg}$$

$$W_r = W\left(\frac{l_1}{L} + \frac{a}{g}\frac{h}{L}\right)$$

(3.44)

$$W_r = 125.6\left(\frac{0.65}{1.2} + \frac{6.5}{9.81}\frac{0.55}{1.2}\right)$$

$$W_r = 106.178 \text{ kg}$$

3.4.2 Weight transfer when cornering

There is weight transfer from the inner to outer wheels when cornering. The rear wheels are affected for a three wheel vehicle with delta configuration.

$$W_{transfer} = \frac{W_r V^2}{gR} * \frac{h}{b}$$

(3.45)

$$W_{transfer} = \frac{106.178 * 8.33^2}{9.81 * 30} * \frac{0.55}{0.64}$$

$$W_{transfer} = 21.51 \text{ kg}$$

3.5 Fabrication

The fabrication of the tricycle involved simple process like manual metal arc welding, bending, cutting, drilling, grinding, riveting and the use of bolts and nuts. The fabrication was made in stages consisting of:

i. The rear carriage and rear axle assembly.
ii. The main chassis
iii. The front fork
iv. The seat

The rear carriage consists of the rear axle, hub mount, rear wheels, hubs, brake calliper and disc, the shock absorber mounts. The rear carriage has an attachment point to the main chassis

that carries a rubber bushing. Other attachment points were provided for shock absorbers. The hub mount is constructed to swivel and has a turnbuckle attached to it used for wheel camber adjustment.

Plate XI: Rear carriage fabrication, February, 2020

The main chassis was made from a 5 cm stainless steel tube. The main tube was shaped by tube bending process and attached to a 3 mm stainless steel angle section which formed the base for attaching the rear end. The steel tube for seat mounting was welded to the main tube. The mounting points for the battery compartment and the controller were welded to the main tube as well. The battery compartment was separately formed with a stainless steel flat bar. Disability leg rest mountings were welded to each end of the stainless steel angle section. The leg rest are detachable and gotten from a wheelchair.

Plate XII: Main chassis, February, 2020

The front fork was removed from a road bicycle frame. It consists of the handle bar, the head tube, the speedometer, and brake levers. The electric wheel motor is mounted to the front fork. It is permanently welded to the main chassis. Additional foot rest were attached to the fork which can be used by people with normal leg function.

Plate XIII: Battery holder, February, 2020

Plate XIV: Foot rest, July, 2021

The seat frame was constructed using a 1 inch stainless steel square tube. Standard bicycle seat springs were attached to provide comfort to the rider. Back rest was attached and adjustable side handles were riveted to the seat. The seat has a wooden base with foam glued to it and all covered with leather.

Plate XV: Seat Fabrication, February, 2020

The tricycle was painted with auto-base paint for a good finish and rust protection. The painting process involved washing to remove oil and dirt, application of body filler and putty to cover creases and kinks and smoothening with sand paper. Primer coat was applied for a thicker finish and then several layers of the cream coloured paint applied.

Plate XVI: Paint work, June, 2021

Plate XVII: Different views of Completed model, July, 2021

3.6 Cost Analysis

Production cost refers to the costs incurred from production of the tricycle. The cost is classified into three: Material cost, labour cost and overhead cost.

The direct material cost is the cost from purchase of materials that are an integral part of the finished product like tyres, stainless steel tubes, and brake callipers. The labour cost is the cost incurred due to labour utilisation in manufacturing the tricycle. This includes but not limited to welding, painting, drilling, and cutting.

The overhead cost includes all production costs not included in direct materials and direct labour. This includes cost of shipment of materials, transportation, cost of items purchased or hired in experiments and tests.

Tables 3.3a and 3.3b gives the breakdown of direct cost of materials involved in the production of the tricycle. Table 3.4 shows the breakdown of labour cost involved while Table 3.5 shows the breakdown of overhead cost involved in the production of the tricycle.

Table 3.3 a: Direct Materials Cost

S/N	Item Description	Quantity	Unit cost (₦)	Total cost (₦)
1	Electric front drive hub motor 1000 W, 48 V	1	76650	76650
2	Controller 1000 W, 48 V	1		
3	Speed LCD Display, 48 V	1		
4	Brake disc and caliper	1		
5	Throttle with reverse function	1		
6	Brake lever	2		
7	Brake disc and caliper	1	2500	2500
8	Brake Cables	2	300	600
9	Bicycle Tires 20 by 2.125, with load rating of 70 kg each, maximum pressure 60 psi	3	1200	2400
10	Lead acid Batteries, 12 V, 7.2 AH	4	5000	20000
11	25 mm stainless steel round tube	4 ft	800	3200
12	30 mm stainless steel round tube	4 ft	800	3200
13	40 mm stainless steel round tube	4 ft	1000	4000
14	20 mm stainless steel square tube	3 ft	1000	3000
15	10 mm steel rod	4 ft	250	1000
16	Stainless steel 1 inch flat bar	4 ft	1000	2000
17	Standard bicycle	1	12000	12000
18	Steel wire 3 mm	1	1200	1200
19	Turnbuckle	1	1500	1500
20	Shock Absorber, DNM 165	2	8750	17500

Table 3.3 b: Direct Materials Cost

S/N	Item Description	Quantity	Unit cost (₦)	Total cost (₦)
21	Rubber Bushings 5mm	2	1000	2000
22	Mud Guard set	2	1200	2400
23	Wheelchair footrest	2	3000	6000
24	Wheelchair arm rest	2	500	1000
25	Foam	1 ft*1 ft	500	500
26	Leather	2 ft*2 ft	500	500
27	Bolt and Nut M10 by 1.5	2	200	400
28	Bolt and Nut M8 by 1.25	4	100	400
29	Bolt and Nut M6 by 1.	4	100	400
30	Cable ties	8	50	400

Direct Material cost is ₦164, 750. 00

Table 3.4: Labour Activities

S/No	Description of work
1	Welding cost
2	Drilling cost
3	Bending cost
4	Painting cost
5	Upholstery work
6	Tyre Assembly work

Labour cost is 30 percent of material cost.

Therefore,

$$Labour\ cost = {}^{30}/_{100} * Material\ cost \quad (3.46)$$

$$Labour\ cost = {}^{30}/_{100} * 164750$$

Labour cost = N49, 425.00

Table 3.5: Overhead Cost

S/No	Item Description	Quantity	Unit cost (₦)	Total cost (₦)
1	Local Transportation		5000	5000
2	Linear String Encoder, CALT CESI, S1000P, 24 VDC for steering angle measurement	1	45500	45500
3	HB961Indicator, for display of steering angle; 24 VDC.	1		
4	Shipment (from overseas) of items: 1-6, 11, 12 and 22.		88250	88250

Overhead cost is ₦138, 750.00

Total Cost = Direct material cost + Labour cost + Overhead cost

Total cost = ₦164, 750. 00 +₦49, 425.00 +₦138, 750.00

Total Cost = ₦352, 925.00

CHAPTER FOUR

4.0 RESULTS AND DISCUSSION

The chapter presents the enhancement of the stability of a disabled tricycle by a well thought-out location of the CG, the wheel base and track dimensions, with aid of steady state cornering equations for handling stability and quasi-static rollover model for rollover stability. In addition, rollover velocity threshold tests were conducted and analysed. Another test was carried out at constant radius in order to determine the understeer gradient using the slope of the steer angle/lateral acceleration curve. The aim of the study is to develop an electric tricycle for the disabled having higher speed and adjustable wheel camber for better handling and lateral stability. Also, the determination of lateral acceleration, lateral acceleration in a turn and during braking that caused rollover were conducted and tested. The detailed steps taken for the research are presented in the subsequent sections of this chapter. Plate XVIII indicates the tricycle with adjustable wheel camber constructed and tested during this study.

Plate XVIII: Tricycle with adjustable wheel camber developed during this project, July, 2021

4.1 Analytical Result

The condition for stability as indicated by equation 3.16 for K≥0 was that the CG was located at L/3 from the rear axle to ensure that the tyres are carrying equal load. The CG position was treated as a design requirement to ensure that condition was met. Consequently, the CG was located longitudinally at 0.55 m from the rear axle to ensure that the front tyre generates a higher cornering coefficient to achieve a positive K_{us} value.

However, it can be seen that during acceleration there was significant transfer of weight from the front to the rear axle. This generated higher normal loads on the rear tyres which resulted to higher lateral loads and slip angles than the front tyre. This likely affected the desired K_{us} value and consequently resulted to poor handling.

The CG height (vertically) was determined to be 0.55 m from the ground. The critical angle was determined experimentally and used in the analysis of equation 3.39. The value was used in the rollover analysis. The C.G height needed to be as low as practically possible to compensate for the vehicle lean due to load transfer in a turn. At a turn of 30 m radius and a velocity of 30 Km/h, the weight transfer from the outer to the inner wheel was evaluated, from equation 3.44, to be 21.51 kg.

In addition, the theoretical examination of the rollover threshold revealed that:

i. As evaluated from equation 3.24 the design satisfied the rollover stability condition.
ii. As evaluated from equation 3.26, the rollover velocity was found to be 34.70 Km/h
iii. While accelerating in a turn, the design failed to meet the requirement for rollover stability as evaluated using equation 3.32
iv. While braking in a turn, the design failed to meet the requirement for rollover stability as evaluated using equation 3.32

4.2 Test Results

Table 4.1 indicated various results of rollover tests performed at various camber angles and turn radii such as actual at 0^o, 5^o, 10^o and 15^o camber respectively. However, these actual figures were compared with the calculated figures.

Table 4.1: Rollover velocities comparison between the calculated and the actual at different wheel camber angles

Radius, *R* (m)	Rollover Velocity, V_{ro} (Km/h),				
	Calculated	Actual at 0^o Camber	Actual at 5^o Camber	Actual at 10^o Camber	Actual at 15^o Camber
5	14.15	6	8	9	9
10	20	9	12	13	14
15	24.52	11	14	15	17
20	28.3	14	15	18	19
25	31.64	17	20	22	24
30	34.70				

The Table 4.1 indicated the rollover velocity threshold significantly increased by applying negative wheel camber. This is indicated by the actual values of the rollover velocity at different camber angles. Conversely, it can be seen that the calculated rollover velocity was significantly lower than the actual values obtained from field test. This can partly be attributed

to the tricycle's transient response when accelerating laterally. The speed of 24 Km/h could not be exceeded during testing. However, rollover velocity was not recorded for the 30 m radius. This is because the 30 m radius test for the rollover velocity, a top speed of 24 Km/h was recorded for all the camber angles with no corresponding risk of rollover. A maximum of 27 Km/h was recorded while carrying out field test on a non-circular path. Plate XIX shown adjustable wheel camber mechanism.

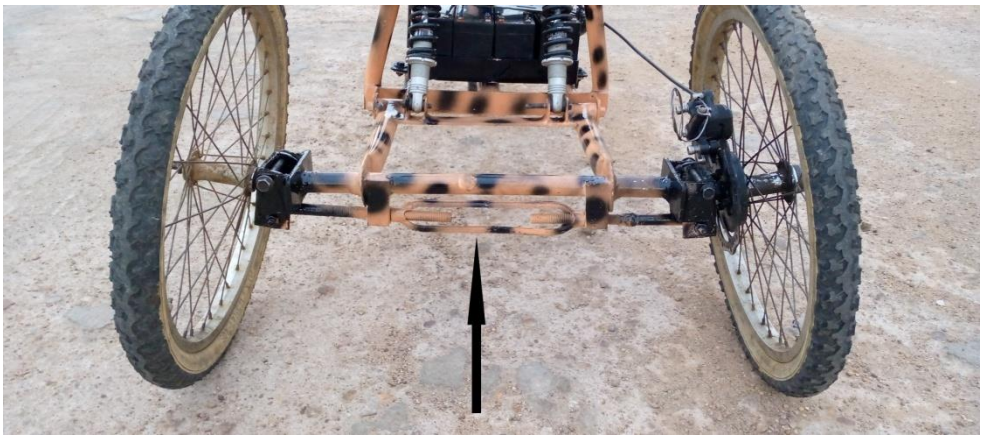

Plate XIX: Wheel camber adjustment mechanism, June, 2021

The results of a constant radius test to determine the tricycle's understeer gradient were indicated in Table 4.2. The steering angle was measured along with the speed and corresponding lateral acceleration.

Table 4.2: Velocity, Lateral Acceleration and The Corresponding Steering Angles

speed Km/h	Lateral acceleration, *ay* (g)	Steering angle, δ			
		δ, at 0° Camber	δ, 5° at Camber	δ, at 10° Camber	δ, at 15° Camber
5	0.01332	5	5	5	5
10	0.05328	5	4	4	4
13	0.09004	2	3	3	3
16	0.13639				0
20	0.21311				
23	0.28185				
27	0.3884				

The result obtained from this test is limited because of the following constraints:

i. A paved surface of 30 m radius, as required for a standard constant radius test is not available.
ii. The tricycle could not attain higher speed required within the limited available paved surface of 15 m radius.

In carrying out the test, a complete circle with a radius of 15 m was used. The highest speed attained at 15 m radius was 17 km/h and the tricycle could not maintain its heading along the circular path. The constant radius test requires the tricycle to attain higher speed than the maximum attained speed of 27 km/h. As a result, the handling response could not be ascertained because the understeer gradient, K, was undetermined.

However, the results showed that the tricycle had a tendency to oversteer at low speeds with relatively low amounts of lateral acceleration, and that it will have poor handling qualities at greater speeds. Plate XX shows the the constant radius test.

Plate XX: Constant radius test, May, 2021

The aim of the electric tricycle study is to bring increased mobility to disabled persons in Nigeria. Presently, hand-powered tricycles are used by many of the disabled in this country, but some current users of the hand-powered tricycles do not have the physical strength or coordination to propel themselves on the tricycle with their arms and hands. The electric tricycle with adjustable wheel camber uses an electric brushless direct current hub motor connected to the front wheel. The motor is powered from a rechargeable battery bank.

Testing was a huge part of this research, since designing for a very real client, it is important that the system be tested to be reliable. Maintenance could not count on it being pampered in

its use. As indicated or explained earlier, the operation of this electric tricycle met its design objectives. Considering the use of available parts and based on the system's reliability, it is decided that the design met the objectives and is appropriate for implementation.

Furthermore, the kinematic bicycle model was modified for use on tricycles with delta design. A constant radius tests with a 15 m radius and different wheel camber angle adjustments of 0^o, 5^o, 10^o and 15^o were performed. At a maximum camber angle of 15^o, only a maximum speed of 17 km/h was achieved without the risk of tipping over at a radius of 15 m. As a result, the understeer gradient could not be determined due to insufficient steering angle measurement and speed readings. For rollover analyses, a quasi-static rollover model was used and rollover test were performed to determine the rollover stability. The tests were performed at various turn radii of 5 m, 10 m, 15 m, 20 m, 25 m and 30 m. and with the wheel camber adjusted to four different angle position (0^o, 5^o, 10^o and 15^o). Wheel camber was found to improve stability, with maximum speeds of 10 km/h at 0^o camber angle and 24 km/h at 15^o camber angle all tested within a 30 m radius turn. It was observed that while camber angle improved stability of the tricycle, the calculated rollover threshold is significantly higher than the actual values.

Tricycle dimensions have a large impact on stability and handling response, as indicated by both tests, however, policy framework is required to regulate usage, design and manufacture to achieve desired user safety.

CHAPTER FIVE

5.0 CONCLUSION AND RECCOMENDATIONS

This study resulted in the development of an electric tricycle with adjustable wheel camber for the disabled. The CG position, wheel base, and wheel track were chosen consciously as design objectives using a steady state cornering equation and a quasi static rollover model. Rollover

stability was studied using different wheel camber angles in rollover tests. A constant radius test was also performed to investigate the tricycle's handling response.

However, the research drawn the following conclusions.

5.1 Conclusion

Tricycle dimensions have a large impact on stability and handling response. Despite the fact that the CG height and longitudinal location were considered as practically as possible for better stability, the very narrow dimensions of the tricycle affected the stability and handling response, as indicated by both tests. As a result, user safety is best achieved by designing stability into the tricycle and policies will be required to serve as a regulatory framework for designers, manufacturers and users. This may take into account classification based on size, user, use of technology, and so on, as well as speed limitations for each class. Speed threshold can be selected for each class through a demonstrated ability to meet specified safety criteria.

The theoretical rollover speed threshold is significantly greater than the practical value. Data from practical tests, such as the one conducted in this study, will assist designers, manufacturers, regulators, and users in making better decisions about the use of such powered tricycles. The turning radius of disabled tricycles, both powered and manual is smaller. As a result, speed restriction mechanisms, as well as the use of wheel camber and other methods of improving stability, are all strongly advised.

The tricycle's rollover stability was greatly improved by using wheel camber. By cambering the wheel negatively, camber thrust acts in the opposite direction of centrifugal force, creating a stabilizing effect. However, this effect reduces the cornering coefficient, which affects the understeer gradient, K, value, and may result in poor steering response. Another reason for the improved rollover stability could be the slight increase in wheel track caused by negative camber.

The results of the constant radius test may indicate poor handling characteristics at higher speeds, which is typical of most three-wheeled vehicles. The angle of the head tube, in particular, affects tricycle handling. This study did not look into steering geometry, which affects tricycle handling.

Designs like this will help people with disability to live a more productive life style and improve their quality of life, to help the nation achieve its social inclusion policy and meet its sustainable development targets.

5.2 Recommendations

Enhancing the safe performance of powered tricycles, including the one developed from this work, still remain a valid objective.

The choice of tyre type to use during design of a tricycle is very significant considering the importance of tire properties and how they affect handling response and rollover stability. The use of fat tyres for bicycle, which is commonly available now, may be considered giving their improved properties. Getting a tire with published properties like cornering stiffness, camber stiffness can help in simplifying the analyses and also facilitate computer simulations.

More refined non-linear models can be used for the analyses such as transient rollover model and equations with higher degree of freedom for the cornering equations to get better result.

The use of lithium-ion batteries will improve the performance of the tricycle. It will enable higher speed, increase range of travel, reduced size and weight reduction. This will get better results for both the rollover test and the constant radius test.

Further recommendations to improve this work could be in areas like:

Research need to be carried out to determine properties of the 20 by 2.125 bicycle tyre and nature of their effect on the stability handling characteristics of the tricycle.

Investigate the steering geometry and its effects on ease of turning, stability and wobble and to explore other options of charging the batteries other than electricity. This could be through the use of solar panels, dynamo, regenerative braking etc.

Carry out structural analysis of the tricycle frame using Finite Element Analysis and also use MATLAB for ride analysis to investigate the suspension response and its effect on the dynamics of the tricycle and rider comfort.

Employ the use of sensors to improve stability through electronic speed control. The motor controller on the tricycle can be modified or developed to use sensors like yaw rate sensors, lateral acceleration sensors to regulate the motor output.

5.3 Contribution to Knowledge

This study added to our understanding by investigating the rollover characteristics and handling response of a disabled tricycle with a very narrow wheel base and wheel track. It was determined that these very narrow tricycles have poor handling characteristics, and that wheel camber improved the tricycle's rollover response. It was also established that user safety cannot be guaranteed solely by factoring stability.

REFERENCES

Abe, M., (2015). Vehicle Dynamics: Theory and Applications, second edition.

Amati, N., Festini, A., Pelizza, L., and Tonoli, A. (2011). "Dynamic modelling and experimental validation of three wheeled tilting vehicles", Vehicle System Dynamics, International Journal of Vehicle Mechanics and Mobility. 49:6, 889-914. doi:10.1080/00423114.2010.503277.

Aripin M.K., Sam Y.M., Kumeresan A.D., Peng K., Hasan M.H.C., Ismail M.F. (2013) A Yaw Rate Tracking Control of Active Front Steering System Using Composite Nonlinear Feedback. In: Tan G., Yeo G.K., Turner S.J., Teo Y.M. (eds) AsiaSim 2013. Asia Sim 2013. Communications in Computer and Information Science, vol 402. Springer, Berlin, Heidelberg. https://doi.org/10.1007/978-3-642-45037-2_22

Ataei, M., Tang, C., Khajepour, A., &Jeon, S. (2019). Active camber system for lateral stability improvement of urban vehicles. *Proceedings of the Institution of Mechanical Engineers, Part D: Journal of Automobile Engineering, 233, 3824 - 3838.*

Austin, E. , Christopher, A. S. , Peter, O. , Saturday, E. W. , & E., D. D. (2015). Determination of Center of Gravity and Dynamic Stability Evaluation of a Cargo-type Tricycle. American journal of mechanical engineering, 3(1), 26-31.

Berote, J.J. (2010). Dynamics and control of a tilting three wheeled vehicle.

Cooper, R.A., (2012). Guest Editorial: Wheelchair research progress, perspectives and transformation. J Rehabil Res Dev; 49(1):1 Retrieved on 17th January, 2019 from https//www.rehab.research.va.gov

Deans, C., (2010). Advanced Composite Design and Manufacture of a Combined Wheelchair and Tricycle. Retrieved on 20 January2019 from www.userweb.eng.gla.ac.uk/

Dressel, A., & Rahman, A., (2011). Measuring Sideslip and Camber Characteristics Of Bicycle Tyres, vehicle system dynamics, 50.8, 1365-1378, DOI: 10.1080/00423114.615408

Ebrahimi A, Kazemi AR, Ebrahimi A. (2016). Wheelchair Design and Its Influence on Physical Activity and Quality of Life Among Disabled Individuals. Iranian rehabilitation journal.; 14(2):85-92. https://doi.org/10.18869/nrip.irj.14.2.8

Edelmann, J., Plöchl, M. &Lugner, P. (2011). Modelling and analysis of the dynamics of a tilting three-wheeled vehicle. MultibodySystDyn 26, 469–487. https://doi.org/10.1007/s11044-011-9258-7

Factsheet: Inclusive & Basic Education For Children With Disabilities In Nigeria: The role of Federal and state Ministries of Education. Retrieved on January 15, 2019 from www.jonapwd.org

Garande, T.A., Sonawane, P.D., Chavan, S., &Barpande, G. (2013). Review of Motorized Tricycle for the Disabled Person.2 *International Journal of Science and Research (IJSR)*

Gillespie, T.D., (1992). Fundamentals of Vehicle Dynamics. SAE *International*

Holcomb, B.D., Klonick, A., Swift, M., & Tran, M. (2009). Making Mobility: Folding Tricycle Attachment for Standard Wheelchairs in Tanzania.

Huston, j., Graves, B., & Johnson, D. (1982). Three Wheeled Vehicle Dynamics. SAE Transactions, 91, 591-604. Retrieved May 27, 2019, from http://www.jstor.org/stable/44631967

J. Ferreira , M. A. Neto , J. P. Nobre , A. M. Amaro , L. M. Roseir. (2014). Multibody dynamic modelling and simulation of a three-wheeled electric car Proceedings of the 9th International Conference on Structural Dynamics, EURODYN

Jeang, A., Liang, F., & Huang, H.F. (2015). Handcycle Design & Development Process for the Disabled.

Jenkins, A., Gooch, S.D., Theallier, D., Dunn, J., (2014). Analysis of a Lever-Driven Wheelchair Prototype and the Correlation between Static Push Force and Wheelchair Performance ,. Proceedings of the 19th World Congress The International Federation of Automatic Control Cape Town, South Africa.

K. Kalyani, R. K., & Kirani, K.S. Power. (2014). Assisted Tricycle with Drive-Train Arrangement for Disabled Persons. International Journal For Research In Applied Science And Engineering Technology. 2(9).

Kooijman, J.D.G., Schwab, A.L., &Meijard, J.P., (2008). Experimental validation of a model of an uncontrolled bicycle. Multibodysystdyn 19, 115-132. https//doi.org/10.1007/s11044-007-9050-x

Leaman, J., and Hung, M.La., (2017) "A Comprehensive Review of Smart Wheelchairs: Past, Present, and Future," in IEEE Transactions on Human-Machine Systems, vol. 47, no. 4, pp. 486-499, doi: 10.1109/THMS.2017.2706727.

Martín Antonio Rodríguez Licea, Edgar Armando Vazquez Rodríguez, Francisco Javier Perez Pinal, Juan Prado Olivares, "The Rollover Risk in Delta Tricycles: A New Rollover Index and Its Robust Mitigation by Rear Differential Braking", Mathematical Problems in Engineering, vol. 2018, Article ID 4972419, 14 pages, 2018. https://doi.org/10.1155/2018/4972419

McLaurin, C., (1990). Current development in wheelchair Research. Retrieved on 17th January, 2019 from https//www.rehab.research.va.gov/momowheelchair/mclaurin/pdf

Md. Shahidul ,I., Zaheed, R., &Nafis, A.(2012). Designing Solar Three-Wheeler for Disable People. International Journal For Research In Applied Science And Engineering Technology. 3(1)

Mukherjee, S., Mohan, D., &Gawade, T., (2004). Rollover Stability Of Three-Wheeled Vehicles.

Muthuganapathy,&R.Bandyopadhyay, S., Adjustable Hand-cranked Tricycle for Mobility Disabled. (2011). 15th National Conference on Machines and Mechanisms NaCoMM2011-188

Nag, P., Panikar, J., Malvankar, M., Pradhan, C., & Chatterjee, S. (1982). Performance evaluation of lower extremity disabled people with reference to hand-cranked tricycle propulsion. *Applied ergonomics, 13 3,* 171-6 .

Park, SJ.,Sohn, JH. (2012). Effects of camber angle control of front suspension on vehicle dynamic behaviors. J MechSciTechnol **26,** 307–313. https://doi.org/10.1007/s12206-011-1206-1

Pineau, J., West, R., Atrash, A., Villemure, J., &Routhier, F. (2011). On the Feasibility of Using a Standardized Test for Evaluating a Speech-Controlled Smart Wheelchair.

Smith, N., (2011). The Face of Disability in Nigeria: A Disability Survey in Kogi and Niger States. Disability, CBR & Inclusive Development, 22(1), pp.35-47. DOI: http://doi.org/10.5463/dcid.v22i1.11

Star, Patrick, J., Prof. (2006). Designing Stable Three Wheeled Vehicles, With Application to Solar Powered Racing Cars. Accessed February 8, 2019, from www.americansolarchallenge.org

Tateishi, Y., Yoshimori, K., Koide, M., & Yamada, K. (1986). The Effects of the Tire Camber Angle on Vehicle Controllability and Stability.

Van Valkenburgh, P., Klein, R., &Kanianthra, J. (1982). Three-Wheel Passenger Vehicle Stability and Handling. SAE Transactions, 91, 605-627. Retrieved June 1, 2019, from http://www.jstor.org/stable/44631968

Visagie, S., Duffield, S., & Unger, M. (2015). Exploring the impact of wheelchair design on user function in a rural South African setting. African journal of disability, 4(1), 171. https://doi.org/10.4102/ajod.v4i1.171

Windes, P., Archibald, M., (2013). Experimental Determination of Bicycle Tire Stiffness. ASEE North central conference 2013, Retrieved on May 16, 2019 From www.people.cst.cmich.ed

Winters, A., (2006). Wheelchair Design in Developing Countries. Accessed on January 5, 2019 from www.web.mit.edu/winter/public

Wong, J.Y., (1993). Theory of ground Vehicles. New York, N.Y.: J. Wiley

Woodruff, A., Surgenor, B., &Knobel, C. (2007). Comparison of Methods to Improve Camber Using a Modelica/Dymola Multi-Body Model. SAE Transactions, 116, 820-826. Retrieved June 3, 2020, from http://www.jstor.org/stable/44687845

World Health Organisation (WHO)., 2017. Powered Two- & Three- Wheeler Safety: A Road Safety Manual For Decision-Makers And Practitioners. Accessed on 18 May, 2019 from www.who.int/publications/i/item/powered-two--and-threewheeler-safety

World health organisation. World report on disability-2011. Retrieved on 17th January, 2019 from https//www.who.intl

Yoshino, T. and Nozaki, H. (2014) Camber Angle Control Method Corresponding to the Electric Vehicle Age. Engineering, **6**, 472-484. doi: 10.4236/eng.2014.68049.

Zandieh, A. (2014). Dynamics of a Three-Wheel Vehicle with Tadpole Design. Retrieved on 01 February, 2019. Fromhttps://www.uwspace.uwaterloo.ca/bitstream/handle.